## REMARKS

### I. Overview

Applicants have reviewed and considered the Office Action dated June 29, 2006. Applicants thank the Examiner for the courtesy extended during the telephonic interview of July 28, 2006. Claims 1 and 2 have been canceled. Claims 3, 4, and 11 have been amended. Support for these amendments can be found in the specification as filed at page 17, line 17 to page 18, line 16 and originally filed claim 1. No new matter has been added. After entry of this amendment, claims 3-11 will be pending in the above-identified application. Applicants respectfully request reconsideration of the above-identified application in view of the amendment and remarks that follow.

### II. Maintained Rejections -35 U.S.C. § 112 – Enablement

Claims 1, 2 and new claims 3-11 stand rejected under 35 U.S.C. § 112, first paragraph, as allegedly failing to comply with the enablement requirement, as set forth previously. The Examiner states protons are the only known activator (agonist) of DEG/ENaC channel proteins. The Examiner states the specification has not taught which agonists would be useful for treating any particular disorder, and nor would agonists be expected to be useful as taught by Waldmann-R et al.

While not acquiescing to the Examiner's arguments, Applicants have removed the term "activating" from claim 11. Claims 1 and 2 have been canceled.

From a telephonic interview, one of the Examiner's concerns seems to be that the claims are not directed towards treating particular conditions associated with the response of acid-sensing ion channels. Applicants have amended claims 3, 4, and 11 so that they now recite

"treating pain caused by activation of acid-sensing ion channels of the DEG/ENaC channel family". Support for this amendment can be found in the specification, at page 17, line 17 to page 18, line 16. Given the evidence of ASIC activation resulting from tissue acidosis in pain in the literature and in the specification, Applicants submit that the skilled artisan could make and use the claimed methods for treating pain caused by ASIC activation. The Examiner appears to agree. As noted by the Examiner, "it is certainly reasonable to expect that specific antagonists of specific DEG/ENaC channel proteins would some day be found and prove useful in the treatment of disorders such as pain and inflammation, as discussed by Waldmann-R et al., at the bottom of page 74". Office Action, at page 3.

The Examiner states that the instant specification provides no teaching of these yet to be found useful compounds. Applicants respectfully remind the Examiner that the present invention is directed to a method of treating pain caused by the activation of ASIC and is not tied to a particular compound for inactivating the ASIC as Examiner seems to suggest.

In response to the Examiner's comments "that the instant specification simply invites that artisan to find such compounds, if indeed they can be found", Office Action, at page 4, Applicants submit that it is quite the contrary. Those of skill in the art have not only identified compounds as discussed in Applicants' specification, but, as disclosed by Applicants, these compounds were shown to have activity in treatment of pain. Applicants submit herewith for the Examiner's consideration three journal articles demonstrating the successful identification of compositions that inhibit ASIC activity using routine techniques, specifically, (1) Dubé et al., Pain. 2005 Sep;117(1-2):88-96; (2) Diochot et al. A New Sea Anemone Peptide, APETx2, Inhibits ASIC3, a Major Acid-sensitive Channel in Sensory Neurons. EMBO J. 2004 Apr

7;23(7):1516-25; (3) Escoubas et al. Isolation of a Tarantula Toxin Specific for a Class of Proton-gated Na+ Channels. J Biol Chem. 2000 Aug 18;275(33):25116-21.

For example, the article authored by Dubé et al. show that their ASIC inhibitor is successful in treating pain in two distinct *in vivo* pain models. Dubé et al., Pain. 2005 Sep;117(1-2):88-96. Dubé et al. report the identification of a non-amiloride blocker A-317567 that is capable of inhibiting ASIC in neurons in a concentration dependent manner. Dubé et al., at page 92, Figure 5. More compelling yet, Dubé et al demonstrate that their compound A-317567, as well as amiloride is efficacious in treating pain in two distinct *in vivo* pain models. Dubé et al., at page 92, Figures 6-7. Importantly, as noted by Dubé et al., A-317567, unlike amiloride, does not interact with renal ENaCs. Dubé et al., at page 93, right column, first paragraph. As another example, the article authored by Escoubas et al. describe the identification and testing of psalmotoxin 1 (PcTX1), a peptide, for its ability to block ASICs using a patch clamp technique and report the peptides ability to specifically block ASIC1a. Escoubas et al., commencing at page 25117, right column, bridging paragraph, and Figure 2. Likewise, Dichot et al. describe the identification and testing of an anemone peptide, APETx2, for its ability to specifically inhibit ASIC3 at pages 1518-1521. Thus, contrary to the Examiner's belief that compounds that specifically inhibit ASIC may not exist, several compounds have been identified using the methods described in the specification. These articles demonstrate that one can obtain and screen compositions and identify compositions that modify ASIC activity.

This is further evidence that Applicants' specification is enabling for methods of treating pain caused by the activation of ASIC proteins involving a step of identifying a composition that inhibits ASIC activity. Moreover, claims drawn to testing and identifying compositions for

ASIC activity have been allowed in the parent application, which does not have a different disclosure than the present invention, and issued in U.S. patent number 6,635,432.

The published journal articles demonstrate that one of skill in the art, relying on the present disclosure and on knowledge in the art at the time the present application was filed, would be able to test compositions and identify a composition capable of inhibiting ASIC for the treatment of pain caused by ASIC activation. Accordingly, the specification and published articles demonstrate that the methods of the invention are enabled for treating pain caused by ASIC activation. In light of the above, Applicants respectfully request that the rejections be withdrawn and reconsidered.

**III. New Rejection Under 35 U.S.C. § 112 – Written Description**

Claims 1-11 are rejected under 35 U.S.C. § 112, first paragraph, as allegedly failing to comply with the written description requirement. The Examiner states the claims require compounds for treating conditions associated with the response of acid-sensing ion channels, yet none are taught in the specification and nor are any known in the art. The Examiner writes that Waldmann-R et al., Ann NY Acad Sci, 30(67-76)1999 state that protons are the only known activator (agonist) of DEG/ENaC channel proteins (ASIC channels), and indicate that activation of these channels contributes to disease state in ischemia and epileptic seizures (page 74); the specification has not taught which agonists would be useful for treating any particular disorder, and nor would agonists be expected to be useful as taught by Waldmann-R et al.

The Examiner states the skilled artisan cannot envision the detailed chemical structure of the required "composition that inhibits, activates or modulates the acid sensing ion channels…in

a therapeutically-effective amount", and therefore conception is not achieved until reduction to practice has occurred, regardless of the complexity or simplicity of the method of isolation.

Applicants respectfully disagree. As an initial matter, Applicants have canceled claims 1 and 2 and amended claim 11 to remove the term "activating". Applicants respectfully submit that the written description standard as applied to this application is improper. As stated: "Adequate description ... does not require the literal support for the claimed invention... Rather, it is sufficient if the originally-filed disclosure would have conveyed to one having ordinary skills in the art that an appellant had possession of the concept of what is claimed." *In Staehelin v. Secher*, 24 USPQ 2d 1513 (BPAI 1992). Furthermore, there is a strong presumption that the adequate written description of the claimed invention is present in the application as filed. MPEP § 2163.03.

The Examiner seems to suggest that only actual reduction to practice, for example, identifying compositions that inhibit ASIC activity, would rise to the level of "possession" of the invention to satisfy the written description requirement. As described above, the specification describes techniques for identifying ASIC inhibitors that enable the user to carry out screening methods and treatments in accordance with the invention.

In so far as the Examiner is relying on *Fiers v. Revel* and *Amgen Inc. v Chugai Pharmaceutical Co. Ltd.* as the bases for this rejection, Applicants note that the cases are not applicable to the present claims. Both *Revel* and *Amgen* involve composition of matter claims, specifically claims to DNA sequences encoding a particular protein. Importantly, Applicants reiterate that they are not claiming an ASIC inhibitor as a composition of matter, much less an ASIC inhibitor identified by the claimed methods, for example, by product by process claim, but instead are claiming methods of use of such inhibitors for treatment of pain. Thus, the claims

here are distinguishable from the situation in the cited cases and *Fiers v. Revel and Amgen Inc. v Chugai Pharmaceutical Co. Ltd.* do not apply.

Applicants reiterate that the claims are not drawn to the compositions themselves. Rather, the method of claim 3 of the present invention comprises identifying a composition for inactivating the current in acid-sensing ion channels of the DEG/ENaC channel family, and thereafter administering such a compound to treat pain. The specification provides ample support for these methods, for example, at pages 19 to 28. Thus, one following the methods of the invention for treating pain caused by activation of ASIC will have a composition available before undertaking to administer it to a subject. Independent claims 4 and 11 recite similar steps.

In view of the arguments above and amendments to the claims, the specification provides an adequate written description of the steps used in the claims. Therefore, Applicants request that the rejections under 35 U.S.C. § 112 be withdrawn and reconsidered.

## IV. Conclusion

Applicant respectfully request that all outstanding rejections be reconsidered and withdrawn. The application is believed to be in a condition for allowance. In the event that the Examiner determines there are other matters to be addressed, Applicants invite the Examiner to contact the undersigned attorney.

Please consider this a one-month extension of time from September 29, 2006 to October 29, 2006 and charge Deposit Account No. 26-0084 in the amount of $60.00. No other fees or extensions of time are believed to be due in connection with this amendment; however, consider this a request for any extension inadvertently omitted, and charge any additional fees to Deposit Account No. 26-0084.

Reconsideration and allowance is respectfully requested.

Respectfully submitted,

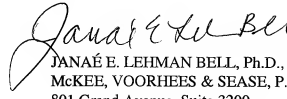

JANAÉ E. LEHMAN BELL, Ph.D., Reg. No. 55,370
McKEE, VOORHEES & SEASE, P.L.C.
801 Grand Avenue, Suite 3200
Des Moines, Iowa 50309-2721
Phone No: (515) 288-3667
Fax No: (515) 288-1338
**CUSTOMER NO: 22885**

Attorneys of Record

- bjh -
Enclosures

Pain 117 (2005) 88–96

PAIN

www.elsevier.com/locate/pain

# Electrophysiological and in vivo characterization of A-317567, a novel blocker of acid sensing ion channels

G.R. Dubé*, Sonya G. Lehto, Nicole M. Breese, Scott J. Baker, Xueqing Wang, Mark A. Matulenko, Prisca Honoré, Andrew O. Stewart, Robert B. Moreland, Jorge D. Brioni

*Abbott Laboratories, Neuroscience Research, Building AP9A—Dept. R4ND,Abbott Park, IL 60064-6118, USA*

Received 29 March 2005; received in revised form 5 May 2005; accepted 23 May 2005

**Abstract**

Acid Sensing Ion Channels (ASICs) are a group of sodium-selective ion channels that are activated by low extracellular pH. The role of ASIC in disease states remains unclear partly due to the lack of selective pharmacological agents. In this report, we describe the effects of A-317567, a novel non-amiloride blocker, on three distinct types of native ASIC currents evoked in acutely dissociated adult rat dorsal root ganglion (DRG) neurons. A-317567 produced concentration-dependent inhibition of all pH 4.5-evoked ASIC currents with an $IC_{50}$ ranging between 2 and 30 μM, depending upon the type of ASIC current activated. Unlike amiloride, A-317567 equipotently blocked the sustained phase of ASIC3-like current, a biphasic current akin to cloned ASIC3, which is predominant in DRG. When evaluated in the rat Complete Freud's Adjuvant (CFA)-induced inflammatory thermal hyperalgesia model, A-317567 was fully efficacious at a dose 10-fold lower than amiloride. A-317567 was also potent and fully efficacious when tested in the skin incision model of post-operative pain. A-317567 was entirely devoid of any diuresis or natriuresis activity and showed minimal brain penetration. In summary, A-317567 is the first reported small molecule non-amiloride blocker of ASIC that is peripherally active and is more potent than amiloride in vitro and in vivo pain models. The discovery of A-317567 will greatly help to enhance our understanding of the physiological and pathophysiological role of ASICs.


*Keywords:* ASIC; Dorsal root ganglia; Amiloride; Pain; Inflammation; Post-operative pain

## 1. Introduction

Tissue damage that leads to either acute or chronic pain is most often associated with varying degrees of localized acidosis (Krishtal, 2003; Reeh and Steen, 1996). Increasing evidence suggests that ASICs, endogenous pH sensors expressed within pain sensory pathways, play an important role in conveying the pain sensation resulting from tissue acidosis (Krishtal, 2003). ASICs are channels primarily permeable to sodium that are quiescent at physiological pH (pH 7.4) but can be activated by mild to moderate drops in ambient pH (half-activation pH between 6.6 and 5.2), causing neurons within pain pathways to become activated (Krishtal, 2003; Waldmann, 2001). For example, subcutaneous injections of an acidified solution caused an amiloride-sensitive pH-dependent increase in pain in healthy human volunteers with a half maximal effect around pH 6.5 and maximal pH of ~5 (Jones et al., 2004; Ugawa et al., 2002). These pH levels are well within the range of those reported for various pathological conditions, e.g. ischemia, inflammation, arthritis, ulcers, and hematomas (Reeh and Steen, 1996). Moreover, it has been shown that inflammatory mediators can lead to an increase in ASIC expression and activity (Mamet et al., 2002; Voilley et al., 2001), further implicating these channels in the pathophysiological response triggered by inflammation.

ASICs are members of a broad family of amiloride-sensitive sodium channels called ENaC/DEG. Six subunits encoded by four genes have now been cloned and

* Corresponding author. Tel.: +1 847 937 2553; fax: +1 847 935 1722.
*E-mail address:* gilles.dube@abbott.com (G.R. Dubé).

0304-3959/$20.00 
doi:10.1016/j.pain.2005.05.021

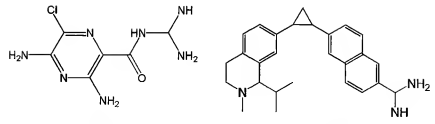


Fig. 1. Chemical structures of amiloride and A-317567.

characterized (ASIC1–4) (Kellenberger and Schild, 2002). Each subunit is composed of two transmembrane domains with intracellular N and C termini. Functional ASICs are thought to be composed of four subunits (homo and heteromultimeric), similar to that described for ENaCs (Firsov et al., 1998). The subunit composition dictates the channels behavior, such as pH sensitivity and response to the reference antagonist amiloride. In DRG neurons, where many subtypes are expressed, native ASICs are reported to be heteromultimeric (Benson et al., 2002). The different pH sensitivity associated with various subunit combinations may provide an exquisite means by which neurons could detect tissue acidosis across a relatively broad range of pH.

To date, the physiological and pathophysiological role of ASICs remain poorly understood, primarily as a result of the lack of suitable pharmacological tools. Amiloride and amiloride-related compounds are the only known small molecule blockers of ASIC. The effects of amiloride are seen at relatively high concentrations; several fold higher than the therapeutic dose required for amiloride-dependent potassium-sparing diuretic effects. We know from animal knockout data that ASIC3 but not ASIC1 null mice failed to develop chronic muscle pain following repeated intramuscular acid injection, suggesting that this subunit plays a central role in this animal model of muscle pain (Sluka et al., 2003). Whether this can be can be observed with pharmacological blockade of ASIC remains to be determined. Here, we describe A-317567 (Fig. 1), a novel non-amiloride compound that can block ASIC current in isolated DRG neurons and that is efficacious in animal models of inflammatory hyperalgesia and post-operative pain.

## 2. Materials and methods

### 2.1. Acute DRG neuron preparation

Adult rat DRG preparation was carried out as previously described (Dubé et al., 2005). All experimental procedures involving rats were conducted under a protocol approved by Abbott Institutional Animal Care and Use Committee. Briefly, adult rats (150–250 g) were deeply anesthetized with $CO_2$ anesthesia and killed by decapitation. Lumbar (L4–L6) DRG were dissected from the vertebral column, cleaned and desheathed in ice-cold Hank's balanced salt solution (HBSS). DRG neurons were incubated in $Ca^{2+}/Mg^{2+}$-free HBSS containing 0.3% collagenase B (Roche Diagnostics Corp., Indianapolis, IN) for 60 min at 37 °C. After washing in fresh HBSS, ganglia were dissociated by trituration using a small-bore plastic transfer pipette. Cells were pelleted by centrifugation, resuspended in DMEM (Gibco, Long Island, NY) supplemented with B27 (Gibco) (1 ml per ganglion), and plated on Biocoat laminin/poly-D-lysine-coated 12 mm glass coverslip (BD Bioscience) at a density of one DRG per coverslip. Cells were maintained in culture for no more than 24 h at 37 °C/5% $CO_2$.

### 2.2. Electrophysiology

Whole cell patch-clamp recordings were obtained from DRG neurons 4–24 h after isolation. Recordings were made at room temperature using an Axon Instruments model 200B patch clamp amplifier with a 1 kHz (8-pole Bessel) low pass filter. Data were digitized at 5 kHz by a Digidata 1322A analog-to-digital converter. Patch pipettes (2–4 MΩ) contained (in mM): 123 potassium gluconate, 7 KCl, 10 HEPES, 8 NaCl, 1 $CaCl_2$, 5 EGTA, 2 Mg-ATP, pH adjusted to 7.25 with KOH. Coverslips were continuously perfused at ~1 ml/min with Tyrode solution containing (mM) 155 NaCl, 5 KCl, 10 HEPES, 10 glucose, 2 $MgCl_2$, 2 $CaCl_2$, pH 7.4 adjusted with NaOH. Access resistance was typically <10 MΩ. All reagents were purchased from Sigma Chemical (St Louis, MO) unless otherwise noted.

Various pH-buffered solutions and drugs of interest were applied to individual cells using a piezoelectric-driven rapid application system (Burleigh Instruments, Fishers, NY). ASIC currents were evoked using 5 s applications of pH 4.5 buffered solution. The effect of the antagonists, A-317567 (C-[6-[2-(1-Isopropyl-2-methyl-1,2,3,4-tetrahydro-isoquinolin-7-yl)-cyclopropyl]-naphthalen-2-yl]-methanediamine) and amiloride (3,5-Diamino-6-chloro-pyrazine-2-carboxylic acid diaminomethyl-amide), were evaluated using co-application with pH 4.5. Dose–response relationships for pH and compounds were obtained by applying buffers of decremental pH (from 7.0 to 4.5) or incremental concentrations of compound in pH 4.5 once every 90 s. For desensitization pH determination, cells were kept in resting pHs ranging from 8.0 to 6.8 for 90 s before activation with pH 4.5 (5 s). Activation, desensitization $pH_{50}$s, and compound potencies were obtained by fitting the concentration response data with a standard logistic equation. ASIC current desensitization kinetics were determined by fitting the decay phase of each pH 4.5-evoked current with a single exponential function ($\tau_{des}$). The amplitude at the end of the pH 4.5 pulse was taken as a measure of the steady-state current and normalized to the peak current ($I_{SS}$). Resensitization kinetics were determined using a paired-pulse

paradigm with increasing interval (from 0.25 to 16 s) using pH 4.5. Recovery results were fitted with a single exponential function ($\tau_{res}$). Statistical comparison of decay rates and $I_{SS}$ between the different current types was done using a one-way ANOVA followed by a Bonferroni post hoc analysis ($P<0.05$). Statistical comparison of fits (dose responses and resensitization kinetics) was done using $F$-test of fit. Statistical analysis was performed using either GraphPad Prism3.0 (GraphPad Software, San Diego, CA USA) or Origin7 (Originlab Corporation, Northhampton MA, USA). All data are expressed as means ± SEM.

## 3. Behavioral assessment

### 3.1. Animals

Adult male Sprague–Dawley rats, 230–350 g (Charles River, Wilmington, MA) were housed in groups of five per cage and given free access to food and water. Animals were maintained on a 12 h light–dark cycle. Animals were only used once in each experiment.

### 3.2. Complete Freund's adjuvant-induced thermal hyperalgesia

Chronic inflammatory hyperalgesia was induced by injecting Complete Freund's Adjuvant (CFA, 50%, 150 μl) into the plantar surface of the right hind paw 48 h prior to testing. For behavioral testing, all animals were placed in Plexiglas chambers ($18\times29\times12.5$ cm$^3$) resting on a temperature-regulated (30 °C) glass surface 30 min before thermal testing. Animals were removed from these chambers for drug or vehicle administration, as described below, and were then returned to their respective chambers. Thermal nociceptive thresholds were determined according to the method described by Hargreaves et al. (1988). Briefly, through the glass surface, a radiant heat source (8 V, 50 W projector bulb) was focused onto the plantar surface of the hind paw. The rat's paw-withdrawal latency to this stimulus was recorded to the nearest 0.1 s. Each animal's latency score was an average of two trials, which were separated by at least 5 min. In all rats, both the ipsilateral and contralateral hind paws were tested. Since withdrawal latencies after injection of vehicle into a hind paw did not differ from latencies observed in uninjected animals (unpublished observations), no vehicle-treated rats were tested.

The mean withdrawal latencies were compared within groups (inflamed vs non-inflamed paws) and between drug- and vehicle-injected groups. In cases of negative values, the scores were designated as 0 (no reversal in hyperalgesia).

### 3.3. Skin incision model of postoperative pain

Paw incision was performed using halothane (2–3%) anesthesia and followed procedures previously described (Brennan et al., 1996). Briefly, the plantar aspect of the left hind paw was placed through a hole in a sterile plastic drape. A 1-cm longitudinal incision was made through the skin and fascia, starting 0.5 cm from the proximal edge of the heel and extending towards the toes, the plantar muscle was elevated and injured longitudinally leaving the muscle origin and insertion points intact. After hemostasis with gentle pressure, the skin was apposed with two mattress sutures of 5-0 nylon.

As previously described (Zhu et al., 2005), hind paw weight bearing (WB) response was assessed using an Incapacitance Analgesia Meter (Stoelting Wood Dale, IL, USA), which is a dual channel scale that separately measures the weight of the animal distributed to each hind paw. While normal rats distribute their body weight equally between the two hind paws (50:50), the discrepancy of weight distribution between an injured and non-injured paw is a reflection of the discomfort level in the injured paw. The rats were placed in the plastic chamber designed so that each hind paw rested on a separate transducer pad. The average was set to record the load on the transducer over a 5 s time period and two numbers displayed represented the distribution of the rat's body weight on each paw in grams (g). For each rat, three readings from each paw were taken and then averaged. Side-to-side WB difference was calculated as the average of the absolute value of the difference between the two hind paws from three trials (right paw reading − left paw reading).

### 3.4. Statistics

All data are expressed as the group mean ± SEM. Statistical significance on group means was measured by an ANOVA, followed by a Fisher's PLSD post hoc analysis ($P<0.05$). $ED_{50}$ values for all experiments were estimated using linear regression.

## 4. Results

We initially surveyed the pH responsiveness of DRG neurons in acutely dissociated adult rat DRG neuron preparations (L4–L6) and found the response profile to vary in frequency and current type according to cell size. At least three broad types of acid-evoked currents were reliably observed in this preparation (Fig. 2); a fast transient current with little steady-state current, a slow desensitizing current, and a fast transient current with a clear steady-state current component. These are referred to here as ASIC1-, 2-, and 3-like currents, respectively, since these had current kinetics, pH activation, and desensitization profiles similar to cloned ASIC1–3. Looking at the respective current properties compiled in Table 1, the three ASIC currents can be clearly differentiated desensitization ($\tau_{des}$) and resensitization ($\tau_{res}$) kinetics. At least one other kind of ASIC current was also observed, but was too infrequent to allow for a thorough characterization. Finally, a fifth kind

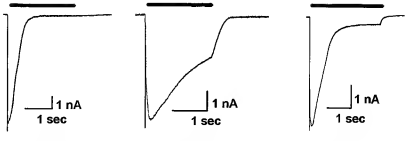


Fig. 2. Different types of ASIC currents can be evoked in adult rat DRG neurons. Rapid application of pH 4.5 buffered saline (horizontal bar) evoked at least three types of current that are differentiated based on their kinetics and pH responsiveness and named based on their relative similarity to the cloned ASICs. (1) ASIC1-like (left) can be described as a relatively fast transient current with little sustained current; (2) ASIC2a-like (middle) was a slow desensitizing current; (3) ASIC3-like current (right) was biphasic with a initial fast transient followed by a well-defined sustained current.

of acid-evoked current, slow non-desensitizing with a sharp deactivation phase was also observed; this current was attributed to the activation of TRPV1 channels and always responded to capsaicin (1 μM, not shown).

Fig. 3 shows the distribution of the three prominent types of ASIC currents across cell sizes in DRG. The biphasic current (ASIC3-like) was the prevalent type of acid-evoked current across all cell sizes. The ASIC1-like current was mostly found in small neurons, sometimes together with TRPV1 currents. The ASIC2-like currents are also more prominent in large neurons. The number of cells without ASIC current (TRPV1-mediated currents and the non-responders) was 52, 43 and 11%, respectively, for small, medium, and large neurons.

### *4.1. Effect of amiloride and A-317567 on acid-evoked current*

The effects of amiloride and A-317567 on ASIC currents were compared. As shown in Fig. 4, co-application of 10 μM amiloride with pH was able to reduce the peak amplitude of each ASIC current evoked by a 5 s application of pH 4.5 to a DRG neuron. On the ASIC3-like current, amiloride had little effect on the sustained part of this current (Fig. 4(C)).

Table 1
Basic properties of different ASIC currents evoked in adult rat DRG neurons

| | ASIC1-like[a] | ASIC2-like[a] | ASIC3-like[a] |
|---|---|---|---|
| Activation $pH_{50}$ | 6.0 (6) | 5.3 (6) | 6.4 (14) |
| Desensitization $pH_{50}$ | 7.3 (3) | None (4) | 7.1 (5) |
| $\tau_{des}$ (ms)[b] | 384±27 (15) | 1762±264 (27)[§] | 366±18 (53) |
| $I_{SS}$ (% of peak)[c] | 2±1 (15)[†] | 33±3 (26)[†] | 15±2 (52)[†] |
| $\tau_{res}$ (s)[d] | 2.6 (4)[‡] | 1.2 (11)[‡] | 1.8 (9)[‡] |

[a] Number of neurons analyzed in parentheses.
[b] One-way ANOVA, $f(2,92)=34.3$, $P<0.01$. *$P<0.05$ vs ASIC1- and 3-like.
[c] One-way ANOVA, $f(2,94)=25.6$, $P<0.01$. †$P<0.05$ across all ASIC types.
[d] Fit comparison across all types: $f(44,141)=4.65$, $P<0.01$. ‡$P<0.05$ across all ASIC types.

Co-application of A-317567 with pH 4.5 resulted in a decrease in the amplitude of the peak of ASIC currents (Fig. 5). However, unlike amiloride, the compound also reduced the sustained portion of ASIC3-like current (Fig. 5(C)). Both amiloride and A-317567 effect were fully reversible (not shown).

To determine the potency of amiloride and A-317567 in our DRG neuron preparation, increasing concentrations of the compounds were sequentially co-applied with pH 4.5. A summary of these results is compiled in Table 2. The potency of amiloride and A-317567 to block ASIC varied according to the type of ASIC current under investigation, and A-317567 was significantly more potent than amiloride for each type of current (Table 2).

### *4.2. In vivo effects of amiloride and A-317567 in two experimental animal models of pain*

To delineate a role for ASIC in pain we first evaluated the analgesic effects of amiloride and A-317567 in Complete Freund's Adjuvant- (CFA-) induced thermal hyperalgesia in rat. As shown in Fig. 6, amiloride showed dose-dependent

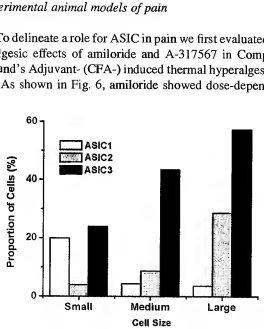


Fig. 3. Distribution of different ASIC currents across cell sizes in adult rat DRG neurons. Percent neurons with ASIC1-, 2-, or 3-like currents in small (<25 μm), medium (25–35 μm) and large (>35 μm) diameter neurons.

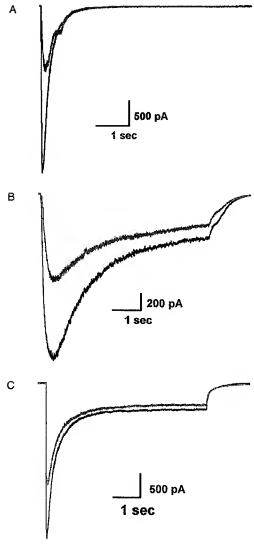


Fig. 4. Amiloride blocks ASIC currents in adult rat DRG neurons. Representative examples of the effect of 10 μM amiloride (co-applied with pH 4.5) on ASIC1-like (top), ASIC2-like (middle) and ASIC3-like (bottom) currents. Black trace is control current evoked with pH 4.5 and the gray trace is the steady state inhibition observed with amiloride.

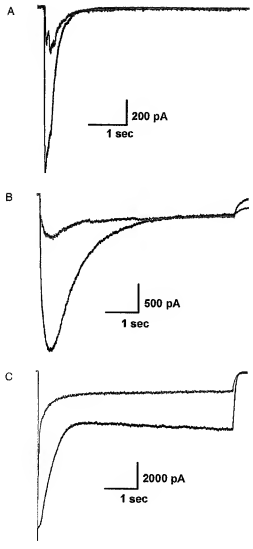


Fig. 5. A-317567 blocks ASIC currents in adult rat DRG neurons. Representative examples of the effect of 10 μM A-317567 (co-applied with pH 4.5) on ASIC1-like (top), ASIC2-like (middle) and ASIC3-like (bottom) currents. Black trace is control current evoked with pH 4.5 and the gray trace is the steady state inhibition observed with A-317567.

efficacy but displayed relatively low potency ($ED_{50}$= 192 μmol/kg, i.p.) in this model. A-317567 was also fully efficacious in the CFA model and was significantly more potent than amiloride ($ED_{50}$=17 μmol/kg, i.p.; $P<0.01$, unpaired *t*-test). There was no significant effect of amiloride or A-317567 on the withdrawal latency of the contralateral paw under these conditions (not shown). We also tested both compounds in the skin incision model, a rat model of post-operative pain that has been shown to have a low tissue pH at the wound (Woo et al., 2004). As shown in Fig. 7, amiloride in this model showed full efficacy and better potency than in the CFA model (70 μmol/kg, i.p.). However, A-317567 was again significantly more potent and also fully efficacious (9 μmol/kg, i.p.; $P<0.01$, unpaired *t*-test). Together, these data support a role for ASIC in pain sensation in acute surgical pain or in more chronic inflammatory pain.

Pharmacokinetic studies were conducted after systemic administration in rats. A-317567 (30 μmol/kg, i.p.) reached

Table 2
Pharmacology of different ASIC currents evoked in adult rat DRG neurons

| | ASIC1-like[a] | ASIC2-like[a] | ASIC3-like[a] |
|---|---|---|---|
| Amiloride $IC_{50}$ (μM) | 30.2 (4) | 51.4 (7) | 37.2 (13) |
| A-317567 $IC_{50}$ (μM)[b] | 2.0 (4)** | 29.1 (6)* | 9.5 (8)** |

[a] Number of neurons analyzed in parentheses.
[b] Fit comparison statistics between amiloride and A-317567 dose–responses: ASIC1 $f(2,36)=36.12$, ASIC2 $f(2,61)=4.37$, ASIC3 $f(2,100)=27.51$. *$P<0.05$., **$P<0.01$.

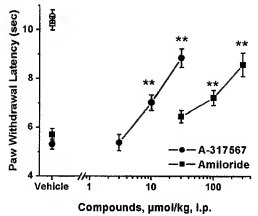


Fig. 6. Dose-dependent analgesic effects of amiloride and A-317567 in the CFA model of chronic inflammatory pain. In vivo dose-dependent reduction of CFA-induced thermal hyperalgesia by amiloride and A-317567 compared to vehicle-treated rats. Both compounds significantly reduced thermal hyperalgesia ($P<0.01$), but A-317567 was 11-fold more potent based on linear regression estimated $ED_{50}$s. Amiloride, A-317567, or vehicle were dosed i.p. 30 min prior to behavioral assessment of thermal sensitivity. Individual data points represent mean ± SEM ($n=12$). $^{**}P<0.01$ compared to control-paired $t$-test.

average plasma levels of 1250 ± 247 ng/ml 30 min after administration, while brain levels were >20-fold lower (52 ± 12 ng/ml). These data indicate that A-317567 has limited brain penetration, and thus is mainly acting peripherally.

Finally, the effect of A-317567 on body fluid homeostasis was evaluated. A-317567 (up to 30 μmol/kg, i.p.) had no significant effect on urine output, and sodium and potassium excretion, and actually decreased urine output at dose higher than those exhibiting analgesic effects (100 μmol/kg; −79.1 ± 56.2%, $n=8$, $P<0.05$ compare to vehicle-treated animals), indicating that this compound does not interact with renal epithelial sodium channels (ENaCs).

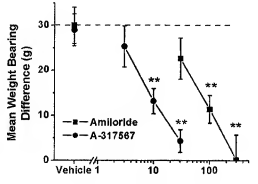


Fig. 7. Dose-dependent analgesic affects of amiloride and A-317567 in the skin incision model of post-operative pain. In vivo dose-dependent reduction of post-operative pain measured as a difference between weight bearing on hind paws 2 h following skin incision surgery to the hind paw by amiloride and A-317567 compared to vehicle-treated rats. Both compounds significantly reduced pain ($P<0.01$), but A-317567 was 7-fold more potent based on linear regression estimated $ED_{50}$s. Amiloride, A-317567, or vehicle were dosed i.p. 30 min prior to behavioral assessment of weight bearing difference. Individual data points represent mean ± SEM ($n=6$). $^{**}P<0.01$ compared to control-paired $t$-test.

## 5. Discussion

ASICs have been hypothesized to play a role in pain transmission in conditions that lead to tissue acidosis. However, this has been difficult to demonstrate due to the lack of pharmacological tools. Here, we characterize both in vitro and in vivo A-317567, the first small molecule non-amiloride ASIC blocker that show appreciable efficacy in two in vivo pain models. In addition to being more potent than amiloride in vivo, A-317567 showed no effect on body fluid homeostasis indicating that unlike amiloride, this compound does not interact with renal ENaCs.

ASICs have been identified in DRG neurons both functionally (Benson et al., 2002; Dirajlal et al., 2003; Petruska et al., 2000), and by microscopy using specific ASIC antibodies or by in situ hybridization (Alvarez de la Rosa et al., 2002; Garcia-Anoveros et al., 2001; Price et al., 2000, 2001; Voilley et al., 2001). Indeed, acid-evoked currents in these cells had been characterized even before the cloning of these channels (Bevan and Yeats, 1991; Krishtal and Pidoplichko, 1981). Collectively, these studies demonstrate that there are many ASIC subtypes expressed in the DRG, contributing to different acid-evoked currents. In the present work, we described several distinguishable types of acid-evoked currents in our lumbar adult rat DRG preparation. While one of these currents can be attributed to the activation of the TRPV1 receptor, at least four types of amiloride-sensitive currents (ASIC currents) were observed. Three of those occurred frequently enough to allow for a thorough characterization (the fourth was only seen twice). All three currents had distinctive properties such as rate of desensitization, and steady state currents in the presence of low pH, activation and desensitization pHs, that allowed for a simple classification. We termed the different responses ASIC1-, ASIC2-, and ASIC3-like, since each type of response displayed overall similarities with cloned homomeric channels (Chen et al., 1998; Lingueglia et al., 1997; Price et al., 1996; Waldmann et al., 1997a,b), but also because ASIC3-like (or DRASIC) is already broadly used in the literature to describe this prominent current in various DRG preparations (e.g. Mamet et al., 2002). However, this terminology should be taken loosely as we have no clear knowledge of the molecular nature of each of these channels. The heterogeneity of acid-evoked response is not unique to our preparation; several reports clearly described similar types of current in their

preparations (Bevan and Yeats, 1991; Dirajlal et al., 2003; Krishtal and Pidoplichko, 1981).

The distribution of each type of response across different neuron sizes indicate that the ASIC1-like response are predominant in small diameter neurons, while the ASIC2- and 3-like are more restricted to larger cells. This is similar to the immunolocalization of ASIC1–3 in DRG (Alvarez de la Rosa et al., 2002), with the difference that ASIC1 is found across all cell sizes. This would indicate that ASIC1 is part of different heteromultioligomer combinations yielding different ASIC current types. This is supported by data from Welsh's lab showing that ASIC3-like current is likely a result of ASIC1–3 combination (Benson et al., 2002; Xie et al., 2002).

Amiloride (and amiloride-related compounds), Psalmotoxin 1, a tarantula peptide that selectively blocks ASIC1a (Escoubas et al., 2000), and APETx2, a sea anemone toxin that selectively blocks ASIC3 (Diochot et al., 2004), are the only ASIC blockers known so far. In the great majority of studies, amiloride has been used to block ASIC, but is a weak blocker, especially in contrast to its affinity for ENaCs (10–100-fold higher) (Benos, 1982; Kleyman and Cragoe, 1988; Palmer, 1992). In our preparation, amiloride was able to block every ASIC response type. We also found that amiloride was efficacious in two different in vivo pain models: CFA-induced thermal hyperalgesia and skin incision model of post-operative pain. Those effects were seen at significantly greater concentration than that needed for amiloride-induced natriuresis and diuresis. The range of potencies seen with amiloride in our pain studies is comparable to that reported elsewhere (Ferreira et al., 1999).

Like amiloride, A-317567 was able to block all ASIC response types with improved potencies over the former. Since this compound is not chemically related to amiloride and was more potent, it provided a unique opportunity to confirm the involvement of ASIC in pain. In both the CFA and skin incision models, A-317567 showed superior potencies over amiloride. The 10-fold improvement is consistent with the shift in potency observed in vitro in our DRG preparation. Furthermore, the lack of natriuretic and diuretic activity with A-317567 suggests that this compound does not interact in ENaCs.

Our current electrophysiological analysis focused exclusively on ASIC currents evoked in DRG neurons. This is well justified in light of the fact that A-317567 displayed extremely poor CNS penetration (Plasma-brain ratio is $<0.05$). However, many ASIC subtypes are expressed throughout the central nervous system, including in dorsal horn neurons (Wu et al., 2004). Furthermore, CFA-induced inflammation has been shown to produce an increase in expression of ASIC1a and 2a subtypes in dorsal-horn (Wu et al., 2004). From the brain/plasma distribution, it seems unlikely that the dorsal horn played a significant role in the analgesic effects of A-317567. However, this possibility cannot be entirely ruled out. This also raises the question of whether additional efficacy/potency would be attained with a peripherally and centrally acting blocker. This may depend upon the type of pain model or pathology being considered.

Our results showing full efficacy of amiloride and A-317567 in the skin incision model is particularly interesting in view of the recent advance in understanding the etiology of this pain model (Woo et al., 2004). In an elegant study, Woo and Colleagues monitored the tissue pH at the site of injury (intraplantar) using a pH-sensitive microelectrode. From intraplantar control pH of 7.16, the pH quickly dropped following skin incision to a value of about 6.9 (10 min post-incision). Incision of the gastrocnemius produced even more pronounce tissue acidosis (down to pH 6.6). Tissue acidosis persisted for several days and was back to control 7 days post-surgery. The pain behaviors were well correlated with tissue pH at the wound. The decrease in pH is paralleled with an increase in extracellular lactate concentration (from 2 to 4 mM) (T. Brennan, 2nd Joint Scientific Meeting of American pain Society and Canadian Pain Society, May 2004). This becomes critical in light of the fact that lactate can potentiate ASIC responses (Immke and McCleskey, 2001). Indeed, it could be argued that the magnitude of the acidosis in the wound may be insufficient to cause significant activation of most ASICs. However, the concomitant accumulation of lactic acid at the site of injury may facilitate ASIC activation.

In healthy human volunteers, transdermal iontophoretic application of protons caused dose-dependent, amiloride-sensitive increase in pain that desensitized over a 5-min period (Jones et al., 2004). Recovery from desensitization was comparatively slow (over several hours). In this study, TRPV1 was found to play only a minor role (Jones et al., 2004). These data, and others (Steen et al., 1995; Ugawa et al., 2002) raise the question as to how a rapid transient sodium current with minimal or no sustained response at pathophysiological pHs such as those reported above can chronically signal pain caused by inflammation or injury. Genetically modified mice lacking or overexpressing specific ASICs have yielded mostly negative results with regards to their role in pain (Drew et al., 2004; Price et al., 2000, 2001; Roza et al., 2004). The exception is the ASIC3 knockout mice that fail to develop chronic muscle pain following repeated acid injection in muscle (Sluka et al., 2003). It will be critical to have the right tools to determine whether similar phenotypes can be observed with the use of a small molecule ASIC blocker such as A-317567.

In summary, A-317567 is a novel non-amiloride ASIC blocker with distinct mode of action and improved potency both in vitro and in vivo over amiloride. While further

evaluation of the mechanism of action of A-317567 is required to fully understand its mode of action, this compound will provide a new tool for investigating ASIC biology, physiology, and pathophysiology.

## Acknowledgements

The authors would like to acknowledge the technical contribution of Jill Welter for the analysis of the plasma and brain distribution of A-317567.

## References

Alvarez de la Rosa D, Zhang P, Shao D, White F, Canessa CM. Functional implications of the localization and activity of acid-sensitive channels in rat peripheral nervous system. Proc Natl Acad Sci USA 2002;99: 2326–31.

Benos DJ. Amiloride: a molecular probe of sodium transport in tissues and cells. Am J Physiol 1982;242:C131–C45.

Benson CJ, Xie J, Wemmie JA, Price MP, Henss JM, Welsh MJ, Snyder PM. Heteromultimers of DEG/ENaC subunits form H+-gated channels in mouse sensory neurons. Proc Natl Acad Sci USA 2002;99: 2338–43.

Bevan S, Yeats J. Protons activate a cation conductance in a sub-population of rat dorsal root ganglion neurons. J Physiol 1991;433: 145–61.

Brennan TJ, Vandermeulen EP, Gebhart GF. Characterization of a rat model of incisional pain. Pain 1996;64:493–501.

Chen CC, England S, Akopian AN, Wood JN. A sensory neuron-specific, proton-gated ion channel. Proc Natl Acad Sci USA 1998; 95:10240–5.

Diochot S, Baron A, Rash LD, Deval E, Escoubas P, Scarzello S, Salinas M, Lazdunski M. A new sea anemone peptide, APETx2, inhibits ASIC3, a major acid-sensitive channel in sensory neurons. EMBO J 2004;23: 1516–25.

Dirajlal S, Pauers LE, Stucky CL. Differential response properties of IB(4)-positive and -negative unmyelinated sensory neurons to protons and capsaicin. J Neurophysiol 2003;89:513–24.

Drew LJ, Rohrer DK, Price MP, Blaver KE, Cockayne DA, Cesare P, Wood JN. Acid-sensing ion channels ASIC2 and ASIC3 do not contribute to mechanically activated currents in mammalian sensory neurons. J Physiol 2004;556:691–710.

Dubé GR, Kohlhaas KL, Rueter LE, Surowy CS, Meyer MD, Briggs CA. Loss of functional neuronal nicotinic receptors in dorsal root ganglion neurons in a rat model of neuropathic pain. Neurosci Lett 2005;376: 29–34.

Escoubas P, De Weille JR, Lecoq A, Diochot S, Waldmann R, Champigny G, Moinier D, Menez A, Lazdunski M. Isolation of a tarantula toxin specific for a class of proton-gated Na+ channels. J Biol Chem 2000;275:25 116–21.

Ferreira J, Santos AR, Calixto JB. Antinociception produced by systemic, spinal and supraspinal administration of amiloride in mice. Life Sci 1999;65:1059–66.

Firsov D, Gautschi I, Merillat AM, Rossier BC, Schild L. The heterotetrameric architecture of the epithelial sodium channel (ENaC) . EMBO J 1998;17:344–52.

Garcia-Anoveros J, Samad TA, Zuvela-Jelaska L, Woolf CJ, Corey DP. Transport and localization of the DEG/ENaC ion channel BNaC1alpha to peripheral mechanosensory terminals of dorsal root ganglia neurons. J Neurosci 2001;21:2678–86.

Hargreaves K, Dubner R, Brown F, Flores C, Joris J. A new and sensitive method for measuring thermal nociception in cutaneous hyperalgesia. Pain 1988;32:77–88.

Immke DC, McCleskey EW. Lactate enhances the acid-sensing Na+ channel on ischemia-sensing neurons. Nat Neurosci 2001;4: 869–70.

Jones NG, Slater R, Cadiou H, McNaughton P, McMahon SB. Acid-induced pain and its modulation in humans. J Neurosci 2004;24: 10974–9.

Kellenberger S, Schild L. Epithelial sodium channel/degenerin family of ion channels: a variety of functions for a shared structure. Physiol Rev 2002;82:735–67.

Kleyman TR, Cragoe Jr EJ. Amiloride and its analogs as tools in the study of ion transport. J Membr Biol 1988;105:1–21.

Krishtal O. The ASICs: signaling molecules? Modulators? Trends Neurosci 2003;26:477–83.

Krishtal OA, Pidoplichko VI. Receptor for protons in the membrane of sensory neurons. Brain Res 1981;214:150–4.

Linguegliа E, de Weille JR, Bassilana F, Heurteaux C, Sakai H, Waldmann R, Lazdunski M. A modulatory subunit of acid sensing ion channels in brain and dorsal root ganglion cells. J Biol Chem 1997; 272:29778–83.

Mamet J, Baron A, Lazdunski M, Voilley N. Proinflammatory mediators, stimulators of sensory neuron excitability via the expression of acid-sensing ion channels. J Neurosci 2002;22:10662–70.

Palmer LG. Epithelial Na channels: function and diversity. Annu Rev Physiol 1992;54:51–66.

Petruska JC, Napaporn J, Johnson RD, Gu JG, Cooper BY. Subclassified acutely dissociated cells of rat DRG: histochemistry and patterns of capsaicin-, proton-, and ATP-activated currents. J Neurophysiol 2000; 84:2365–79.

Price MP, Snyder PM, Welsh MJ. Cloning and expression of a novel human brain Na+ channel. J Biol Chem 1996;271:7879–82.

Price MP, Lewin GR, McIlwrath SL, Cheng C, Xie J, Heppenstall PA, Stucky CL, Mannsfeldt AG, Brennan TJ, Drummond HA, Qiao J, Benson CJ, Tarr DE, Hrstka RF, Yang B, Williamson RA, Welsh MJ. The mammalian sodium channel BNC1 is required for normal touch sensation. Nature 2000;407:1007–11.

Price MP, McIlwrath SL, Xie J, Cheng C, Qiao J, Tarr DE, Sluka KA, Brennan TJ, Lewin GR, Welsh MJ. The DRASIC cation channel contributes to the detection of cutaneous touch and acid stimuli in mice. Neuron 2001;32:1071–83.

Reeh PW, Steen KH. Tissue acidosis in nociception and pain. Prog Brain Res 1996;113:143–51.

Roza C, Puel JL, Kress M, Baron A, Diochot S, Lazdunski M, Waldmann R. Knockout of the ASIC2 channel in mice does not impair cutaneous mechanosensation, visceral mechanonociception and hearing. J Physiol 2004;558:659–69.

Sluka KA, Price MP, Breese NM, Stucky CL, Wemmie JA, Welsh MJ. Chronic hyperalgesia induced by repeated acid injections in muscle is abolished by the loss of ASIC3, but not ASIC1. Pain 2003;106: 229–39.

Steen KH, Issberner U, Reeh PW. Pain due to experimental acidosis in human skin: evidence for non-adapting nociceptor excitation. Neurosci Lett 1995;199:29–32.

Ugawa S, Ueda T, Ishida Y, Nishigaki M, Shibata Y, Shimada S. Amiloride-blockable acid-sensing ion channels are leading acid sensors expressed in human nociceptors. J Clin Invest 2002;110: 1185–90.

Voilley N, de Weille J, Mamet J, Lazdunski M. Nonsteroid anti-inflammatory drugs inhibit both the activity and the inflammation-induced expression of acid-sensing ion channels in nociceptors. J Neurosci 2001;21:8026–33.

Waldmann R. Proton-gated cation channels–neuronal acid sensors in the central and peripheral nervous system. Adv Exp Med Biol 2001;502: 293–304.

Waldmann R, Bassilana F, de Weille J, Champigny G, Heurteaux C, Lazdunski M. Molecular cloning of a non-inactivating proton-gated Na+ channel specific for sensory neurons. J Biol Chem 1997a;272: 20975–8.

Waldmann R, Champigny G, Bassilana F, Heurteaux C, Lazdunski M. A proton-gated cation channel involved in acid-sensing. Nature 1997b;386: 173–7.

Woo YC, Park SS, Subieta AR, Brennan TJ. Changes in tissue pH and temperature after incision indicate acidosis may contribute to post-operative pain. Anesthesiology 2004;101:468–75.

Wu LJ, Duan B, Mei YD, Gao J, Chen JG, Zhuo M, Xu L, Wu M, Xu TL. Characterization of acid-sensing ion channels in dorsal horn neurons of rat spinal cord. J Biol Chem 2004;279:43716–24.

Xie J, Price MP, Berger AL, Welsh MJ. DRASIC contributes to pH-gated currents in large dorsal root ganglion sensory neurons by forming heteromultimeric channels. J Neurophysiol 2002;87:2835–43.

Zhu CZ, Hsieh G, El-Kouhen O, Wilson SG, Mikusa JP, Hollingsworth PR, Chang R, Moreland RB, Brioni J, Decker MW, Honore P. Role of central and peripheral mGluR5 receptors in post-operative pain in rats. Pain 2005;114:195–202.

THE JOURNAL OF BIOLOGICAL CHEMISTRY
© 2000 by The American Society for Biochemistry and Molecular Biology, Inc.

Vol. 275, No. 33, Issue of August 18, pp. 25116–25121, 2000
Printed in U.S.A.

# Isolation of a Tarantula Toxin Specific for a Class of Proton-gated $Na^+$ Channels*

Received for publication, April 28, 2000, and in revised form, May 16, 2000
Published, JBC Papers in Press, May 26, 2000, DOI 10.1074/jbc.M003643200

**Pierre Escoubas‡**, Jan R. De Weille‡, Alain Lecoq§, Sylvie Diochot‡, Rainer Waldmann‡, Guy Champigny‡, Danielle Moinier‡, André Ménez§, and Michel Lazdunski‡¶**

*From the ‡Institut de Pharmacologie Moléculaire et Cellulaire, Centre National de la Recherche Scientifique, 660 route des Lucioles, Sophia-Antipolis, 06560 Valbonne, France, **the Université Pierre et Marie Curie, Paris 75006, France, and the §Département d'Ingéniérie des protéines, CEA, Saclay 91130, France*

**Acid sensing is associated with nociception, taste transduction, and perception of extracellular pH fluctuations in the brain. Acid sensing is carried out by the simplest class of ligand-gated channels, the family of $H^+$-gated $Na^+$ channels. These channels have recently been cloned and belong to the acid-sensitive ion channel (ASIC) family. Toxins from animal venoms have been essential for studies of voltage-sensitive and ligand-gated ion channels. This paper describes a novel 40-amino acid toxin from tarantula venom, which potently blocks ($IC_{50}$ = 0.9 nM) a particular subclass of ASIC channels that are highly expressed in both central nervous system neurons and sensory neurons from dorsal root ganglia. This channel type has properties identical to those described for the homomultimeric assembly of ASIC1a. Homomultimeric assemblies of other members of the ASIC family and heteromultimeric assemblies of ASIC1a with other ASIC subunits are insensitive to the toxin. The new toxin is the first high affinity and highly selective pharmacological agent for this novel class of ionic channels. It will be important for future studies of their physiological and physio-pathological roles.**

Proton-gated $Na^+$-permeable channels are the simplest form of ligand-gated channels. They are present in many neuronal cell types throughout the central nervous system (1–5), suggesting an important function of these channels in signal transduction associated with local pH variations during normal neuronal activity. These channels might also play an important role in pathological situations such as brain ischemia or epilepsy, which produce significant extracellular acidification. They are also present in nociceptive neurons (1–3, 5, 6) and are thought to be responsible for the sensation of pain that accompanies tissue acidosis in muscle and cardiac ischemia (7, 8), corneal injury (9), and inflammation and local infection (10, 11). It is only very recently that the first proton-gated channel, acid-sensitive ion channel (ASIC)[1] was cloned (12). The ASICs belong to a superfamily that includes amiloride-sensitive epithelial $Na^+$ channels (13, 14), the FMRFamide-gated $Na^+$ channel (15), and the nematode degenerins (DEGs), which probably correspond to mechano-sensitive $Na^+$-permeable channels (16). Several ASIC subunits have now been described: ASIC1a (12), ASIC1b (17), ASIC2a (18–21), ASIC2b (22), and ASIC3 (23–25). The different subunits produce channels with different kinetics, external pH sensitivities, and tissue distribution. They can form functional homomultimers as well as heteromultimers (21, 22, 26). ASIC1a and ASIC1b both mediate rapidly inactivating currents following rapid and modest acidification of the external pH. However, although ASIC1a is present in both brain and afferent sensory neurons, its splice variant ASIC1b is found only in sensory neurons (17). ASIC2a forms an active $H^+$-gated channel and is abundant in the brain but essentially absent in sensory neurons, whereas its splice variant ASIC2b is present in both brain and sensory neurons and is inactive as an homomultimer. ASIC2b can form functional heteromultimers with other ASIC subunits and particularly ASIC3 (21). ASIC3 is found exclusively in small sensory neurons that act as nociceptors. Its expression in various heteromultimeric systems generates a biphasic current with a fast inactivating phase followed by a sustained component (22). The association of ASIC2b with ASIC3 forms an heteromultimer with properties (time course and ionic selectivity) similar to those of a native sustained $H^+$-sensitive channel, which is present in dorsal root ganglion cells and appears to play a particularly important role in pain sensation (6).

Venoms from snakes, scorpions, sea anemones, marine snails, and spiders are rich sources of peptide toxins that have proven of great value in the functional exploration of voltage-sensitive and ligand-gated ion channels. This report describes the discovery and characterization from the venom of the South American tarantula *Psalmopoeus cambridgei*, of psalmotoxin 1 (PcTX1), the first potent and specific blocker of this new class of ASIC channels.

## EXPERIMENTAL PROCEDURES

*Venom and Toxin Purification—P. cambridgei (Araneae Theraphosidae)* venom was obtained by electrical stimulation of anesthetized spiders (Invertebrate Biologics). Freeze-dried crude venom was resuspended in distilled water, centrifuged (14,000 rpm, 4 °C, 20 min), filtered on 0.45-μm microfilters (SJHVL04NS, 4-mm diameter; Millipore), and stored at −20 °C prior to analysis. Crude venom diluted to 10 times the initial volume was fractionated by C8 reversed-phase high pressure liquid chromatography (RP-HPLC) (10 × 250 mm, 5C8MS; Nacalai Tesque) using a linear gradient of acetonitrile/water in constant 0.1% trifluoroacetic acid. A second purification step used cation exchange chromatography on a Tosoh SP5PW column (4.6 × 70 mm) (Tosoh), with a linear gradient of ammonium acetate in water (20 mM to 2 M). A total of 160 μl of venom was purified in two separate batches (10 and 150 μl). All solvents used were of HPLC grade. Separation was conducted on a Hewlett-Packard HP1100 system coupled to a diode array detector and a microcomputer running the Chemstation® software.

* This work was supported by the Center National de la Recherche Scientifique and the Association Française contre les Myopathies. The costs of publication of this article were defrayed in part by the payment of page charges. This article must therefore be hereby marked "*advertisement*" in accordance with 18 U.S.C. Section 1734 solely to indicate this fact.

¶ To whom correspondence should be addressed. Tel.: 33-4-93-95-77-02; Fax: 33-4-93-95-77-04; E-mail: ipmc@ipmc.cnrs.fr.

[1] The abbreviations used are: ASIC, acid-sensitive ion channel; PcTX1, psalmotoxin 1; RP, reversed-phase; HPLC, high pressure liquid chromatography; DRG, dorsal root ganglion; Fmoc, *N*-(9-fluorenyl)-methoxyearbonyl.

Monitoring of the elution was done at 215 and 280 nm.

*Peptide Characterization*—Samples were hydrolyzed in a Waters Pico-Tag station, with 6 N HCl (0.6% phenol) at 110 °C, under vacuum for 20 h. Hydrolyzed peptides were derivatized with phenylisothiocyanate, and the derivatized amino acid mixtures were analyzed by C18 RP-HPLC using a gradient of 60% acetonitrile in 50 mM phosphate buffer (100 mM $NaClO_4$). The peptide was reduced and alkylated by 4-vinyl-pyridine, desalted by C8 RP-HPLC, and submitted to automated N-terminal sequencing on an Applied Biosystems model 477A gas phase sequencer.

Reduced-alkylated toxin was submitted to the following treatments: (*a*) tosylphenylalanyl chloromethyl ketone-treated Trypsin (Sigma), 2% w/w at 37 °C for 14 h in 100 mM ammonium bicarbonate, 0.1 mM $CaCl_2$, pH 8.1; (*b*) V8 protease at 37 °C for 24 h in 50 mM ammonium bicarbonate, pH 7.8, in 10% acetonitrile; and (*c*) BNP-skatole (2-(nitrophenylsulfenyl)-3-methyl-3-bromoindolenine) at 37 °C for 24 h in 75% acetic acid. Resulting peptides were separated by RP-HPLC using a linear gradient of acetonitrile/water in constant 0.1% trifluoroacetic acid.

Mass spectra of native PcTX1 dissolved in α-cyano-4-hydroxycinnamic acid matrix were recorded on a MALDI-TOF Perseptive Voyager Elite spectrometer (Perseptive Biosystems), in positive ion linear mode using an internal calibration method with a mixture of β-insulin (3495.9 Da) and bovine insulin (5733.5 Da). Data were analyzed using the GRAMS386 software. Theoretical molecular masses and pI values were calculated from sequence data using the GPMAW protein analysis software. Synthetic PcTX1 was analyzed on a Micromass Platform II electrospray system (Micromass, Altrincham, UK), in positive mode (cone voltage 20kV, temperature 60 °C).

Sequence homologies were determined using sequences obtained from a search of nonredundant protein data bases *via* the BLAST server. Sequence alignments and percentages of similarity were calculated with ClustalW.

*Peptide Synthesis and Refolding*—The synthesis of native PcTX1 was performed using the Fmoc/*tert*-butyl and maximal temporary protection strategy on an Applied Biosystems 433A synthesizer. The chemical procedure used 0.05 mM of Fmoc-Thr(OBu)-4-hydroxymethylphenoxy resin (0.39 mmol/g), a 20-fold excess of each amino acid, and dicyclohexylcarbodiimide/1-hydroxy-7-azabenzotriazole activation. Deprotection (1.5 h) and cleavage (200 mg of peptide + resin) were achieved using 10 ml of a mixture trifluoroacetic acid/triisopropylsilane/water (9.50:225, v/w/v). The acidic mixture was then precipitated twice in 100 ml of cold diethylether. The solid was dissolved in 50 ml of 10% aqueous acetic acid and freeze-dried. The crude reduced toxin was purified by RP-HPLC on a C18 semi-preparative column (21 × 250 mm, Jupiter) using a 40-min gradient of acetonitrile/water in 0.1% trifluoroacetic acid (0–18% B in 4 min, 30% B in 30 min, and 100% B in 6 min, where B is 90% acetonitrile/$H_2O$/0.1%trifluoroacetic acid).

Oxidation of the reduced toxin was achieved at 0.1 mg/10 ml in degassed potassium phosphate buffer (100 mM, pH 7.8) using the redox couple reduced glutathione (5 mM)/oxidized glutathione (0.5 mM). The disappearance of the reduced peptide was monitored by RP-HPLC on a C18 analytical column (10 × 15 mm, Vydac) using a 40-min gradient (0–18% B in 8 min, 30% B in 18 min, and 60% B in 14 min).

*Expression in Xenopus Oocytes*—Cloning of cDNA and synthesis of complementary RNA were done as described previously (26). *Xenopus laevis* were purchased from Centre de Recherches en Biochimie Macromoléculaire (Montpellier, France). Pieces of the ovary were surgically removed, and individual oocytes were dissected in a saline solution (ND96) containing 96 mM NaCl, 2 mM KCl, 1.8 mM $CaCl_2$, 2 mM $MgCl_2$, and 5 mM HEPES (pH 7.4 with NaOH). Stage V and VI oocytes were treated for 2 h with collagenase (1 mg/ml, type Ia; Sigma) in ND96 to remove follicular cells. cRNA (ASIC1a, ASIC2a, Kv2.1, and Kv2.2) or DNA (ASIC1b, rnASIC3, Kv4.2, and Kv4.3) solutions were injected (5–10 ng/μl for cRNA and 50–100 ng/μl for DNA, 50 nl/oocyte) using a pressure microinjector. The oocytes were kept at 19 °C in the ND96 saline solution supplemented with gentamycin (5 μg/ml). Oocytes were studied within 2–4 days following injection. In a 0.3-ml perfusion chamber, a single oocyte was impaled with two standard glass microelectrodes (1–2.5 MΩ resistance) filled with 3 M KCl and maintained under voltage clamp using a Dagan TEV 200 amplifier. Stimulation of the preparation, data acquisition, and analysis were performed using the pClamp software (Axon Instruments). All experiments were performed at room temperature (21–22 °C) in ND96. 0.1% bovine serum albumine was added in solutions containing PcTX1 to prevent its adsorption to tubing and containers. For measurements of ASIC currents, changes in extracellular pH were induced by rapid perfusion, with or without PcTX1, near the oocyte. Test solutions with a pH of 4 or 5 were buffered with MES rather than HEPES. Voltage-dependent $K^+$ channels were activated by depolarization tests to +10 mV from a holding potential of −80 mV, and the toxin solutions were applied externally by gently puffing 100 μl near the oocyte.

In the initial screening, 1-μl aliquots of crude venoms were tested at a 1:1000 dilution in ND96 solution. During the fractionation process aliquots (1:20) of chromatographic fractions were dried, redissolved in ND96, and applied to the oocyte by perfusion.

*Expression in COS Cells*—COS cells, at a density of 20,000 cells/35-mm diameter Petri dish, were transfected with a mix of CD8 and one of the following plasmids: pCI-ASIC1a, pCI-ASIC1b, pCI-ASIC2a, and pCI-ASIC3 (1:5) using the DEAE-Dextran method. Cells were used for electrophysiological measurements 1–3 days after transfection. Successfully transfected cells were recognized by their ability to fix CD8 antibody-coated beads (Dynal, Norway).

*DRG Neurons Cultures and Cerebellar Granule Cell Cultures*—DRG of 2–3-day-old Wistar rats were mechanically dissociated and maintained in culture in Eagle's medium supplemented with 100 ng/ml nerve growth factor. Cells were used for electrophysiological recordings 2 or 3 days after plating.

Cerebella of 4–8-day-old mice were dissected, mechanically dissociated, and cultured as described previously (27). Cells were used for electrophysiological recordings 10–14 days after plating.

*Electrophysiology on COS Cells and Neurons*—Ion currents were recorded using either the whole cell or outside-out patch clamp technique, and results were stored on hard disc. Data analysis was carried out using the Serf freeware. Statistical significance of differences between sets of data was estimated by the single-sided Student test. The pipette solution contained 140 mM KCl, 2 mM $MgCl_2$, 5 mM EGTA, and 10 mM HEPES (pH 7.2). The bath solution contained 140 mM NaCl, 5 mM KCl, 2 mM $MgCl_2$, 2 mM $CaCl_2$, and 10 mM HEPES (pH 7.3). Changes in extracellular pH were induced by shifting one of six outlets of a microperfusion system in front of the cell or patch. Experiments were carried out at room temperature (20–24 °C).

## RESULTS

*Purification*—The screening of several tarantula venoms was carried out against cloned ASIC channels expressed in *Xenopus* oocytes. It singled out *P. cambridgei* venom as containing a potent inhibitor of the ASIC1a proton-gated current. A diluted solution of 1 μl of crude venom (1:1000) applied to the oocyte provoked a 90% block of the ASIC1a current. Bioassay-guided fractionation of the venom by reversed-phase and cation exchange chromatography led to the purification of the minor venom constituent Psalmotoxin 1 (PcTX1), in a two-step process (Fig. 1, *A* and *B*). PcTX1 is a 40-amino acid peptide, possessing 6 cysteines linked by three disulfide bridges. Its full sequence was established by N-terminal Edman degradation of the reduced alkylated toxin and of several cleavage fragments (Fig. 1*D*). The calculated molecular mass (4689.40 Da average) was in accordance with the measured molecular mass (4689.25 Da) and suggested a free carboxylic acid at the C-terminal extremity.

PcTX1 has limited overall homology to other spider venom toxins identified to date (Fig. 1*E*). However, it shares a conserved cysteine distribution (Fig. 1*F*) found both in spider venom and cone snails polypeptide toxins (28, 29). It is a basic polypeptide (pI 10.38 for the native form with disulfide bridges bonded) comprising a large number of basic residues (9 residues, including 4 arginines) but also of acidic residues (6 residues).

*Synthesis*—The chemical synthesis of PcTX1-OH unambiguously confirmed the structure of PcTX1. The purified refolded synthetic toxin (PcTX1 *s*) and the native form have identical measured molecular mass, and when co-injected in two separate experiments using reversed-phase and cation exchange HPLC, native and synthetic PcTX1 were indistinguishable in their migration and co-eluted in both systems (Fig. 1*C*). Most electrophysiological experiments were therefore conducted with the synthetic toxin.

*Selective Block of ASIC1a*—The effect of PcTX1 on the activity of ASIC1a, ASIC1b, ASIC2a, and ASIC3 channels expressed in *X. laevis* oocytes is shown in Fig. 2. The natural as well as

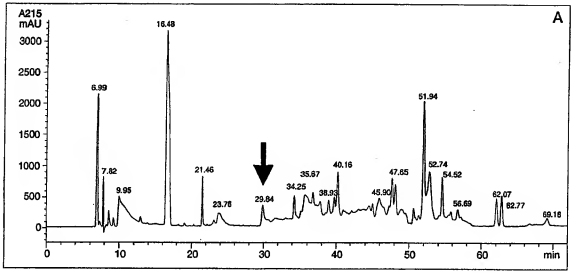


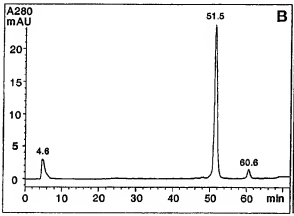


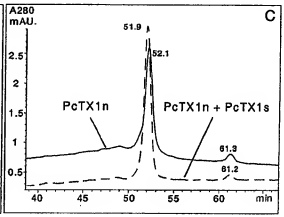


D

```
PcTX1          EDCIPKWKGCVNRHGDCCEGLECWKRRRSFEVCVPKTPKT
Edman          ----------------------------X------>
BNP-skatole                              KRRRSFEVCVPKTPKT
Trypsin No7                              XXEVCVP
V8                                         VCVPKTPKT
```

E

```
                                                          % Sim  Activity
PcTX1          ----EDCIPKWKGCVNRHG-DCCEGLECWKRRRSFEVCVPKTPKT-          ASIC1a
HpTX2          ----IDCGKLESCGDTNA--DCCEGYVCRL------WCKLDW----  59.5  Kv4.2
HaTX1          -----ECRYLWGCGKTTS--DCCKHLGCKFS----DKYCAWDFTFG-  59.8  Kv2.1
SNX482         GVDKACKRYMSCGCSVND--DCCPRLGCHSL---ESYCAWDLTFSD  60.0  VSCC (R)
GsTXS1A        -----DCVRFWGKCSQTS--DCCPHLACKSRW-PRNICVWTGSV--  68.9  VSCC (P/N)
PaTX1          -----YCQKWMWTCDSAR--KCCEGLVCRL------WCKKII----  55.6  Kv4.2/4.3
```

F

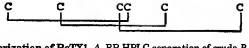


FIG. 1. **Purification and characterization of PcTX1.** *A*, RP-HPLC separation of crude *P. cambridgei* venom (10 μl) with a linear gradient of water/acetonitrile in 0.1% aqueous trifluoroacetic acid. The *arrow* indicates fraction 10, which containing PcTX1. *B*, cation exchange chromatography of fraction 10 with a linear gradient of ammonium acetate (20 mM to 2 M in 88 min). *C*, co-elution experiments with the native toxin (PcTX1n, *solid trace*) injected alone (100 pmol) and co-injected with the synthetic toxin (PcTX1n + PcTX1 s, *dotted trace*, 100 pmol each) by cation exchange HPLC. *D*, PcTX1 sequence determination by automated Edman degradation of reduced-alkylated peptide and proteolytic cleavage fragments. *E*,

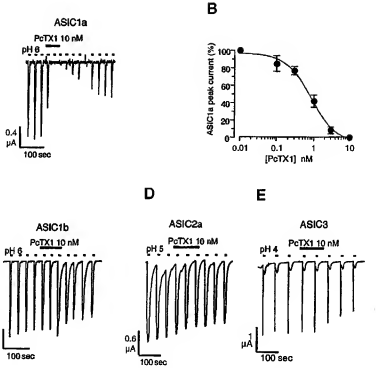


**Fig. 2. PcTX1 selectively blocks $H^+$-gated channels expressed in oocytes.** *A*, complete inhibition of the ASIC1a current by 10 nM PcTX1. Oocytes were clamped at −60 mV, and currents were activated by a pH drop from pH 7.4 to pH 6 (*short bars*) every 30 s. The reversibility of the blockade was observed during extensive washout. *B*, dose-response curve for synthetic PcTX1 block of the ASIC1a current activated by a pH drop from pH 7.4 to pH 6. Points represent the means ± S.E. (4–7 experiments). $IC_{50}$ = 0.9 nM, $n_H$ (Hill coefficient) = 1.2. *C*, the ASIC1b current was activated by a pH drop from pH 7.4 to pH 6 every 30 s. The *black bar* indicates a 2-min perfusion of PcTX1 (10 nM, $n$ = 5). The incomplete reversibility is due to a rundown of the $Na^+$ current, which is observed under repetitive stimulations by consecutive pH drops at 30-s intervals. *D*, ASIC2a current activated by a drop to pH 5 every 45 s. The *black bar* indicates a 2 min perfusion of PcTX1 (10 nM, $n$ = 9). *E*, the rapid and slow components of the ASIC3 current are activated at pH 4 every min. The *black bar* indicates a 2-min perfusion of PcTX1 (10 nM, $n$ = 3).

the synthetic toxin block the ASIC1a current recorded at pH 6, with an $IC_{50}$ of 0.9 nM (Fig. 2, *A* and *B*). The blockade is rapid and reversible. PcTX1 at 10 nM also completely blocks the ASIC1a current activated by a pH drop to pH 5 or pH 4 (not shown). PcTX1 is highly selective. Neither the native nor the synthetic PcTX1 (10 nM or 100 nM) blocked ASIC1b currents activated at pH 6 (Fig. 2*C*). Similarly, the ASIC2a channel activated at a pH drop to pH 5 was insensitive to the action of PcTX1 at 10 nM (Fig. 2*D*) or 100 nM (not shown). The rapid and slow components of the ASIC3 channel were also insensitive to the perfusion of PcTX1 at 10 nM (Fig. 2*E*) and 100 nM (not shown). The toxin was also tested on the epithelial $Na^+$ channel formed by the assembly of $\alpha$, $\beta$, and $\gamma$ subunits (30), and no inhibition occurred with concentrations of 10 nM or 100 nM PcTx1 ($n$ = 3, not shown).

Sequence homologies of PcTX1 with other spider toxins that block different subtypes of voltage-dependent $K^+$ channels such as hanatoxins (Kv2.1) (31), heteropodatoxins (Kv4.2) (32), and phrixotoxins (Kv4.2, Kv4.3) (33) (Fig. 1*E*) prompted us to test its effects against Kv2.1, Kv2.2, Kv4.2, and Kv4.3 channels expressed in *Xenopus* oocytes. These channels were not affected by 10 or 100 nM PcTX1 (not shown).

Experiments carried out with the same ASIC channels expressed in COS cells confirmed the results obtained in oocytes. ASIC1a was completely inhibited by 10 nM PcTX1, whereas ASIC1b, ASIC2a, and ASIC3 were insensitive ($n$ = 10 for each channel) to a higher toxin concentration of 50 nM (not shown).

PcTX1 was then assayed on heteromultimers of the ASIC1a subunit (Fig. 3). Co-expression of ASIC1a and ASIC3 in COS cells produces a rapidly inactivating $H^+$-gated current ($\tau$ = 0.19 ± 0.01 s at pH 6, $n$ = 5) that is insensitive to PcTX1 ($n$ = 10) (Fig. 3*C*), whereas ASIC1a homomultimers produce a current that inactivates more slowly at the same pH ($\tau$ = 2.10 ± 0.30 s, $n$ = 10) but that is completely blocked by PcTX1 (10 nM) (Fig. 3*A*). ASIC1a/ASIC2a heteromultimers were also insensitive to PcTX1 (Fig. 3*B*).

The ASIC1a channel can also be blocked by amiloride, but the $IC_{50}$ is 10 $\mu$M (12), *i.e.* $10^4$ times lower in affinity than PcTX1. Moreover amiloride is not selective. It blocks the transient current generated by ASIC1a (12), ASIC1b (17), ASIC2a (18, 19), and ASIC3 (23).

*Activity of PcTX1 on Native Proton-gated Currents*—Small DRG neurons isolated from 2-day-old rats were voltage clamped at −60 mV and stimulated by a pH drop from pH 7.3 to pH 6. As previously observed in small sensory neurons from trigeminal ganglia (1), this pH change evoked three different types of responses that are presented in Fig. 4 (*A–C*). Currents presented in Fig. 4*A* were blocked by 3–10 nM of the toxin PcTX1, whereas $H^+$-evoked currents in other neurons were insensitive to the toxin (Fig. 4, *B–C*). DRG neurons express at least two subpopulations of transient currents as judged by their constants of inactivation (Fig. 4, *A*, *B*, and *D*). One population inactivates very rapidly with a time constant of inactivation below 0.5 s, whereas the other one has time constants between 1 and 3 s, the average time constant of inactivation being 1.95 ± 0.14 s ($n$ = 23). The data clearly indicate that the most rapidly inactivating currents with an average time constant of inactivation of 0.24 ± 0.03 s ($n$ = 22) are insensitive to PcTX1. Only the more slowly inactivating $H^+$-gated channels are highly sensitive to PcTX1.

The dose-response curve presented in Fig. 4*E* was obtained from the PcTX1-sensitive population of neurons. The $IC_{50}$

multiple sequence alignment of PcTX1 and short spider peptides of similar structure and known mode of action. % *Sim*, percentage of similarity, identical + homologous residues. *Black boxes* indicate conserved residues, and *gray boxes* indicate functionally homologous residues. *X* indicates undetermined residues, and *bold type* indicates residues confirmed by cleavage peptide sequencing. *F*, conserved cysteine positions and disulfide bridges arrangement by homology to known toxins. Sequences are from Ref. 32 (HpTX2), Ref. 37 (SNX482), Ref. 33 (PaTX1), Ref. 31 (HaTX1), and Ref. 38 (GsTX3IA). *VSCC*, voltage-sensitive calcium channels; *Kv*, voltage-dependent potassium channels. All peptides except HpTX2 are from tarantula venoms.

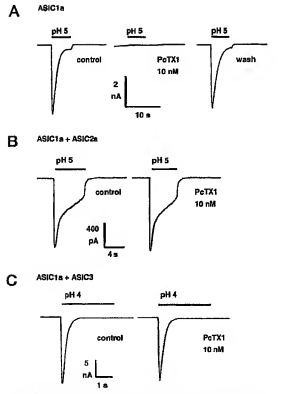


FIG. 3. **Effect of PcTX1 on ASIC homomultimers and heteromultimers.** PcTX1 blocks ASIC1a homomultimers and is inactive on ASIC1a/ASIC2a and ASIC1a/ASIC3 heteromultimers. COS cells transfected with ASIC1a, ASIC1a + ASIC2a, or ASIC1a + ASIC3 were voltage clamped at −60 mV and subjected to a pH drop as indicated ($n$ = 10). Although ASIC1a homomultimers were inhibited by 10 nM PcTX1 (*A*), none of the heteromultimers were sensitive to the toxin (*B* and *C*). Note that the sustained component produced by ASIC3 homomultimers (Fig. 2*E*) is absent in the ASIC1a + ASIC3 heteromultimer (*C*).

value for half-maximum inhibition is 0.7 nM, very similar to the value of 0.9 nM obtained for ASIC1a channels expressed in *Xenopus* oocytes.

Fig. 4*F* shows that a change of the extracellular pH from pH 7.3 to pH 6 in neurons that express the channel type shown in Fig. 4*A* evokes a rapid depolarization resulting in a train of action potentials. This effect is blocked by very low concentrations of PcTX1, and this inhibition is reversible.

ASIC channel subunits are highly expressed in cerebellum and particularly in granular cells (12, 34). This is why we have used these cells to analyze the properties of these channels in central nervous system neurons (Fig. 5). Cerebellar granule cells in culture all responded to a pH drop from pH 7.3 to pH 6 with a transient $Na^+$ inward current characterized by a time constant of inactivation of 2.06 ± 0.17 s ($n$ = 10) (Fig. 5*A*). Both the rate of inactivation and the pH dependence of this $H^+$-gated $Na^+$ channel ($pH_{0.5}$ 6.6 *versus* $pH_{0.5}$ 6.4) are very similar to those of the ASIC1a channel (Ref. 12 and this work) (Fig. 5*B*). $H^+$-gated $Na^+$ channels with the same properties have been recently identified in cortical neurons (35). The transient $H^+$-gated $Na^+$ channel expressed by granule cells was completely inhibited by 10 nM PcTX1 ($n$ = 10) (Fig. 5*A*).

## DISCUSSION

PcTX1 is a novel toxin from tarantula venom that is a potent and specific blocker of one class of $H^+$-gated $Na^+$ channels. The molecular scaffold of PcTX1 is likely to be similar to that previously described for both cone snail and spider toxins (28,

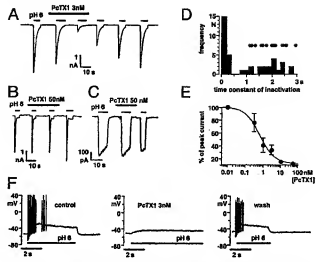


FIG. 4. **Effect of PcTX1 on DRG neurones.** PcTX1 inhibits a subpopulation of $H^+$-gated currents in dorsal root ganglion neurons. $H^+$-gated currents were recorded from DRG neurons in the whole cell voltage clamp configuration. Neurons were clamped at −60 mV, and currents were evoked by rapid jumps in pH from pH 7.3 to pH 6 (*short bars* above the traces in *A–D*). In 23 of 48 $H^+$-responsive neurons PcTX1 inhibited the $H^+$-gated current (*A*), whereas very rapidly inactivating or very slowly inactivating currents recorded in 25 other $H^+$-responsive neurons were resistant to 50 nM of the toxin (*B* and *C*). Current inactivation in each cell expressing either $H^+$-gated currents as in *A* or *B* was fitted with a single exponential, and the profile showing the distribution of time constants in the different cells is shown in *D*. The time constants of the currents that could be inhibited by PcTX1 are shown in the same graph as *filled circles*. *E*, dose inhibition curve obtained from cells expressing the PcTX1-sensitive channels (as in *A*), $IC_{50}$ = 0.7 nM. *F*, DRG neurons (in current clamp) respond to a drop in extracellular pH from pH 7.3 to pH 6, with a burst of spike activity, which is suppressed by PcTX1.

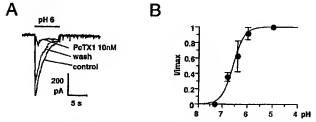


FIG. 5. **PcTX1 inhibits the $H^+$-gated current in cerebellar granule cells.** Mouse cerebellar granule cells were voltage clamped at −60 mV and subjected to a drop in pH from pH 7.3 to pH 6. Almost all of the current is inhibited by 10 nM PcTX1 (*A*). The pH dependence of the proton-gated current in cerebellar cells is shown in *B*.

36). It comprises a triple-stranded antiparallel β-sheet structure reticulated by three disulfide bridges and tightly folded into the "knottin" fold pattern (29). PcTX1 is characterized by the unusual quadruplet $Lys^{25}$-$Arg^{26}$-$Arg^{27}$-$Arg^{28}$, which probably forms a strongly positive "patch" at the surface of the toxin molecule, constituting an area that is a strong candidate for receptor recognition.

It is particularly intriguing to observe (*a*) that PcTX1 is absolutely specific for ASIC1a and can distinguish between the two ASIC1 splice variants ASIC1a and ASIC1b, although they only differ in their N-terminal sequence (17); (*b*) that PcTX1 can also distinguish between ASIC1a, ASIC2 and ASIC3; and (*c*) that PcTX1 looses its capacity to block ASIC1a as soon as this subunit is associated with another member of the family, be it ASIC2a or ASIC3.

An important site of the interaction of ASIC1a with PcTX1 is probably located in the extracellular stretch of 113 amino acids

situated immediately after the first transmembrane domain. This is the only extracellular site where the splice variants ASIC1a and ASIC1b are different. They are identical in extracellular regions except for the 113-residue region immediately C-terminal to the first transmembrane domain.

ASIC1a is present in the central nervous system (notably in the hippocampus and the cerebellar granular layer) as well as in DRG neurons (12). Electrophysiological experiments have shown that both cerebellar granule cells and a subpopulation of DRG neurons possess $H^+$-gated currents that inactivate at pH 6 with time constants of 1.95–2.06 s, very similar if not identical to the time constant of inactivation ($2.10 \pm 0.30$ s) of the homomultimeric ASIC1a current expressed in COS cells. The $H^+$-gated currents in these neurons are inhibited by very low concentrations of PcTX1. The resemblance in the inactivation kinetics and pH dependence, in the selective block of the current by PcTX1 and the near identity of the $IC_{50}$ values for the blockade of ASIC1a channels ($IC_{50} = 0.9$ nM) and of native channels ($IC_{50} = 0.7$ nM) strongly suggest that the $H^+$-gated current with a $\tau_{inact}$ of ~2 s in both DRG cells and cerebellar granular cells is mediated by an homomultimeric assembly of ASIC1a. This view is strengthened by the fact that none of the heteromultimeric channels tested (ASIC1a/ASIC2a and ASIC1a/ASIC3) is sensitive to the toxin.

DRG neurons also express $H^+$-gated currents with time constants of inactivation that are either faster or slower than the time constant of inactivation of the homomultimeric ASIC1a current. A class of these proton-sensitive channels inactivates at a fast rate ($\tau_{inact} = 0.24 \pm 0.03$ s), which turns out, as shown in this work, to be very similar to the rate of inactivation of the ASIC1a/ASIC3 channel expressed in COS cells ($\tau_{inact} = 0.19 \pm 0.01$ s). This rapidly inactivating current, like the current generated by ASIC1a/ASIC3 heteromultimers, is insensitive to PcTX1.

The ASIC3 channel alone or in association with ASIC2b (22) probably corresponds to the sustained current recorded in DRG cells (6). ASIC3 homomultimers, ASIC3/ASIC2b heteromultimers, and the native noninactivating $H^+$-gated channels are not blocked by PcTX1. It is hoped that further studies will provide other toxins specifically active on these maintained channels that are thought to play an important role in pain (6).

Spider venoms are mixtures of neuroactive peptides capable of incapacitating the prey through a myriad of molecular mechanisms. PcTX1 is a potent tool that now opens the way to a more detailed analysis of the physiological function of the important class of $H^+$-gated $Na^+$ channels.

*Acknowledgments*—We are grateful to M. Jodar, Y. Benhamou and V. Lopes for technical assistance and to E. Linguelgia for the epithelial $Na^+$ channel and ASIC2b clones and very helpful discussions. The support of Dr. T. Nakajima and the Suntory Institute for Bioorganic Research (Osaka, Japan) is gratefully acknowledged.

## REFERENCES

1. Krishtal, O. A., and Pidoplichko, V. I. (1981) *Neurosci. Lett.* **24,** 243–246
2. Krishtal, O. A., and Pidoplichko, V. I. (1981) *Brain Res.* **214,** 150–154
3. Krishtal, O. A., and Pidoplichko, V. I. (1981) *Neuroscience* **6,** 2599–2601
4. Davies, N. W., Lux, H. D., and Morad, M. (1988) *J. Physiol. (Lond.)* **400,** 159–187
5. Akaike, N., and Ueno, S. (1994) *Prog. Neurobiol.* **43,** 73–83
6. Bevan, S., and Yeats, J. (1991) *J. Physiol. (Lond.)* **433,** 145–161
7. Benson, C. J., Eckert, S. P., and McCleskey, E. W. (1999) *Circ. Res.* **84,** 921–928
8. Pan, H. L., Longhurst, J. C., Eisenach, J. C., and Chen, S. R. (1999) *J. Physiol. (Lond.)* **518,** 857–866
9. Chen, X., Gallar, J., and Belmonte, C. (1997) *Invest. Ophthalmol. Vis. Sci.* **38,** 1944–1953
10. Kress, M., and Zeilhofer, H. U. (1999) *Trends Pharmacol. Sci.* **20,** 112–118
11. McCleskey, E. W., and Gold, M. S. (1999) *Annu. Rev. Physiol.* **61,** 835–856
12. Waldmann, R., Champigny, G., Bassilana, F., Heurteaux, C., and Lazdunski, M. (1997) *Nature* **386,** 173–177
13. Linguelgia, E., Voilley, N., Waldmann, R., Lazdunski, M., and Barbry, P. (1998) *FEBS Lett.* **318,** 95–99
14. Canessa, C. M., Horisberger, J. D., and Rossier, B. C. (1993) *Nature* **361,** 467–470
15. Linguelgia, E., Champigny, G., Lazdunski, M., and Barbry, P. (1995) *Nature* **378,** 730–733
16. Huang, M., and Chalfie, M. (1994) *Nature* **367,** 467–470
17. Chen, C. C., England, S., Akopian, A. N., and Wood, J. N. (1998) *Proc. Natl. Acad. Sci. U. S. A.* **95,** 10240–10245
18. Waldmann, R., Champigny, G., Voilley, N., Lauritzen, I., and Lazdunski, M. (1996) *J. Biol. Chem.* **271,** 10433–10436
19. Price, M. P., Snyder, P. M., and Welsh, M. J. (1996) *J. Biol. Chem.* **271,** 7879–7882
20. Garcia-Anoveros, J., Derfler, B., Neville-Golden, J., Hyman, B. T., and Corey, D. P. (1997) *Proc. Natl. Acad. Sci. U. S. A.* **94,** 1459–1464
21. Champigny, G., Voilley, N., Waldmann, R., and Lazdunski, M. (1998) *J. Biol. Chem.* **273,** 15418–15422
22. Linguelgia, E., de Weille, J. R., Bassilana, F., Heurteaux, C., Sakai, H., Waldmann, R., and Lazdunski, M. (1997) *J. Biol. Chem.* **272,** 29778–29783
23. Waldmann, R., Bassilana, F., de Weille, J., Champigny, G., Heurteaux, C., and Lazdunski, M. (1997) *J. Biol. Chem.* **272,** 20975–20978
24. De Weille, J. R., Bassilana, F., Lazdunski, M., and Waldmann, R. (1998) *FEBS Lett.* **433,** 257–260
25. Babinski, K., Le, K. T., and Seguela, P. (1999) *J. Neurochem.* **72,** 51–57
26. Bassilana, F., Champigny, G., Waldmann, R., de Weille, J. R., Heurteaux, C., and Lazdunski, M. (1997) *J. Biol. Chem.* **272,** 28819–28822
27. Lauritzen, I., De Weille, J., Adelbrecht, C., Lesage, F., Murer, G., Raisman-Vozari, R., and Lazdunski, M. (1997) *Brain Res.* **753,** 8–17
28. Narasimhan, L., Singh, J., Humblet, C., Guruprasad, K., and Blundell, T. (1994) *Nat. Struct. Biol.* **1,** 850–852
29. Norton, R. S., and Pallaghy, P. K. (1998) *Toxicon* **36,** 1573–1583
30. Canessa, C. M., Merillat, A. M., and Rossier, B. C. (1994) *Am. J. Physiol.* **267,** C1682–C1690
31. Swarts, K. J., and Mackinnon, R. (1995) *Neuron* **15,** 941–949
32. Sanguinetti, M. C., Johnson, J. H., Hammerland, L. G., Kelbaugh, P. R., Volkmann, R. A., Saccomano, N. A., and Mueller, A. L. (1997) *Mol. Pharmacol.* **51,** 491–498
33. Diochot, S., Drici, M. D., Moinier, D., Fink, M., and Lazdunski, M. (1999) *Br. J. Pharmacol.* **126,** 251–263
34. Waldmann, R., and Lazdunski, M. (1998) *Curr. Opin. Neurobiol.* **8,** 418–424
35. Varming, T. (1999) *Neuropharmacology* **38,** 1875–1881
36. Pallaghy, P. K., Nielsen, K. J., Craik, D. J., and Norton, R. S. (1994) *Protein Sci.* **3,** 1833–1839
37. Newcomb, R., Szoke, B., Palma, A., Wang, G., Chen, X., Hopkins, W., Cong, R., Miller, J., Urge, L., Tarcsy-Hornoch, K., Loo, J. A., Dooley, D. J., Nadasdi, L., Tsien, R. W., Lemos, J., and Miljanich, G. (1998) *Biochemistry* **37,** 15353–15362
38. Lampe, R. A., Defeo, P. A., Davison, M. D., Young, J., Herman, J. L., Spreen, R. C., Horn, M. B., Mangano, T. J., and Keith, R. A. (1993) *Mol. Pharmacol.* **44,** 451–460

The EMBO Journal (2004) 23, 1516–1525 | © 2004 European Molecular Biology Organization | All Rights Reserved 0261-4189/04
www.embojournal.org

THE EMBO JOURNAL

# A new sea anemone peptide, APETx2, inhibits ASIC3, a major acid-sensitive channel in sensory neurons

**Sylvie Diochot, Anne Baron, Lachlan D Rash, Emmanuel Deval, Pierre Escoubas, Sabine Scarzello, Miguel Salinas and Michel Lazdunski***

Institut de Pharmacologie Moléculaire et Cellulaire, Centre National de la Recherche Scientifique, Institut Paul Hamel, Sophia Antipolis, Valbonne, France

**From a systematic screening of animal venoms, we isolated a new toxin (APETx2) from the sea anemone *Anthopleura elegantissima*, which inhibits ASIC3 homomeric channels and ASIC3-containing heteromeric channels both in heterologous expression systems and in primary cultures of rat sensory neurons. APETx2 is a 42 amino-acid peptide crosslinked by three disulfide bridges, with a structural organization similar to that of other sea anemone toxins that inhibit voltage-sensitive $Na^+$ and $K^+$ channels. APETx2 reversibly inhibits rat ASIC3 ($IC_{50}$ = 63 nM), without any effect on ASIC1a, ASIC1b, and ASIC2a. APETx2 directly inhibits the ASIC3 channel by acting at its external side, and it does not modify the channel unitary conductance. APETx2 also inhibits heteromeric ASIC2b + 3 current ($IC_{50}$ = 117 nM), while it has less affinity for ASIC1b + 3 ($IC_{50}$ = 0.9 μM), ASIC1a + 3 ($IC_{50}$ = 2 μM), and no effect on the ASIC2a + 3 current. The ASIC3-like current in primary cultured sensory neurons is partly and reversibly inhibited by APETx2 with an $IC_{50}$ of 216 nM, probably due to the mixed inhibitions of various co-expressed ASIC3-containing channels.**

*The EMBO Journal* (2004) **23**, 1516–1525. doi:10.1038/sj.emboj.7600177; Published online 25 March 2004
*Subject Categories*: membranes & transport; neuroscience
*Keywords*: ASIC3; channel; sea anemone; toxin

## Introduction

Acid-sensing ion channels (ASICs) are $H^+$-gated $Na^+$-permeable channels formed by the homo- or heteromeric association of six different subunits (Waldmann and Lazdunski, 1998): ASIC1a (Waldmann *et al*, 1997b), ASIC1b (Chen *et al*, 1998), ASIC2a (Price *et al*, 1996; Waldmann *et al*, 1996), ASIC2b (Lingueglia *et al*, 1997), ASIC3 (Waldmann *et al*, 1997a; de Weille *et al*, 1998; Babinski *et al*, 1999), and ASIC4 (Akopian *et al*, 2000; Grunder *et al*, 2000). Only ASIC1a, ASIC1b, ASIC2a, and ASIC3 are functionally activated by extracellular $H^+$ when expressed alone. ASIC2b can modulate heteromeric ASIC currents by inducing a sustained nonselective cation current following the transient peak (Lingueglia *et al*, 1997; Coscoy *et al*, 1999).

In sensory neurons, ASIC currents have been implicated in pain transduction associated with acidosis in inflamed or ischemic tissues (Reeh and Steen, 1996; Waldmann and Lazdunski, 1998; Benson *et al*, 1999; Kress and Zeilhofer, 1999; Pan *et al*, 1999; Sutherland *et al*, 2001; Voilley *et al*, 2001; Mamet *et al*, 2002; Ugawa *et al*, 2002; Krishtal, 2003), particularly ASIC3, which is mainly expressed in sensory neurons (Waldmann *et al*, 1997a; Voilley *et al*, 2001). Recent studies in knockout mice confirm that ASIC3 plays a major role in high-intensity pain stimuli (Price *et al*, 2001; Chen *et al*, 2002) and in acid-induced hyperalgesia (Sluka *et al*, 2003). An involvement in the mechanosensitivity of large sensory neurons has also been proposed (Xie *et al*, 2002).

Further analysis of the involvement of ASIC3 in the electrical activity of nociceptors requires selective pharmacological tools. To date, the repertoire of active ligands on the ASIC3 channel is limited to amiloride, nonsteroidal anti-inflammatory drugs, and $Gd^{3+}$ (Waldmann *et al*, 1997a; Babinski *et al*, 2000; Voilley *et al*, 2001) that act as inhibitors, and to the mammalian neuropeptides NPFF and NPSF that activate ASIC3 (Askwith *et al*, 2000; Deval *et al*, 2003). However, none of these drugs is absolutely specific for ASIC channels.

In the past 25 years, animal venoms have yielded a great number of toxins that modulate specifically and with high affinity voltage-gated $Na^+$, $K^+$, and $Ca^{2+}$ currents (Moczydlowski *et al*, 1988; Norton, 1991; Harvey *et al*, 1994; Uchitel, 1997; Tytgat *et al*, 1999; Escoubas *et al*, 2000b), $Ca^{2+}$-gated $K^+$ channels (Hugues *et al*, 1982; Shakkottai *et al*, 2001), and mechano-sensitive $K^+$ channels (Bode *et al*, 2001). Recently, *Conus* toxins have been shown to target neurotransmitter receptors at sensory synapses (England *et al*, 1998). The only toxin known to affect ASIC channels is Psalmotoxin 1 (PcTx1), a tarantula venom peptide that acts as a potent and specific inhibitor of homomeric ASIC1a channels (Escoubas *et al*, 2000a; Escoubas *et al*, 2003). We report here the identification of APETx2, a novel peptide toxin isolated from sea anemone venom, which selectively inhibits homomeric ASIC3 channels as well as the ASIC1a + 3, ASIC1b + 3, and ASIC2b + 3 heteromers. A physico-chemical characterization of APETx2 is presented, including its disulfide bridge arrangement, and a structural model based on its homology with the $K^+$ channel sea anemone toxin BDS-I. We show that APETx2 inhibits ASIC3-like currents recorded from rat sensory neurons. APETx2 thus constitutes the first pharmacological tool to analyze the physiological involvement of ASIC3-containing channels in neuronal excitability and pain coding.

*Corresponding author. Institut de Pharmacologie Moléculaire et Cellulaire, Centre National de la Recherche Scientifique, UMR 6097, Institut Paul Hamel, 660, Route des Lucioles, Sophia Antipolis, 06560 Valbonne, France. Tel.: +33 493 957702 or 03; Fax: +33 493 957704; E-mail: ipmc@ipmc.cnrs.fr

**Received: 12 December 2003; accepted: 25 February 2004; published online: 25 March 2004**

## Results

### *Purification of an ASIC3 inhibitory peptide from Anthopleura elegantissima*

In order to find effectors of the ASIC3 channel, a large number of scorpion, bee, spider, snake, and sea anemone venoms (1/1000 dilution) or peptide fractions (0.1 mg/ml) were screened on ASIC3 channels expressed in *Xenopus* oocytes. A peptide fraction from the sea anemone *Anthopleura elegantissima* (Bruhn *et al*, 2001) was found to inhibit more than 80% of the rat ASIC3 current stimulated at pH6. The active peptide was purified to homogeneity by bioassay-guided reversed-phase and cation-exchange chromatography (Supplementary Figure A), and was named APETx2.

### *Biochemical properties*

APETx2 is a basic peptide (pI = 9.59) of 42 amino acids, crosslinked by three disulfide bridges and has a calculated 280 nm molecular absorbance of $\varepsilon_{280} = 11170$. Its full sequence was established by N-terminal Edman degradation, and its measured monoisotopic mass (4557.96 Da) was in perfect accordance with the mass calculated from sequence data (4557.88 Da, accuracy 17.5 ppm), indicating a free C-terminal carboxylic acid. APETx2 displays 64% sequence identity (76% homology) with APETx1 (Diochot *et al*, 2003) (Figure 1A) and only 34% sequence identity (57 and 55% homology, respectively) with the BDS-I and BDS-II toxins from *Anemonia sulcata*, which inhibit the voltage-dependent $K^+$ (Kv) channel Kv3.4 (Diochot *et al*, 1998). Sequence identity with $Na^+$ channel activators such as AP-A, AP-B, AP-C, APE1-1, and APE-2 from *Anthopleura* sp (Bruhn *et al*, 2001) is only 25–29% (homology 41–47%). APETx2 does not display any sequence homologies with the ASIC1a inhibitor PcTx1 previously isolated from a tarantula venom (Escoubas *et al*, 2000a).

The determination of disulfide bridges in small peptide toxins is crucial to understand and confirm the three-dimensional structure of the toxins. Partial reduction and cyanylation of APETx2 yielded five components separated by HPLC (Supplementary Figure B). MALDI-TOF MS indicated that peaks 2 and 3 predominantly contained singly reduced/cyanylated isoforms (+52 Da). Based on its sequence homology and conserved cysteine spacing with BDS-I, APETx2 was predicted to have similar disulfide pairing. Figure 1B shows the predicted fragments and calculated masses for each disulfide bond of APETx2 and the masses observed from the cleavage of singly reduced isoforms in HPLC peaks 2 and 3. Following cleavage and full reduction, MALDI-TOF MS analysis revealed that peak 2 contained only one singly reduced isoform with the major ions (*m/z* 2025.53 and 2097.53), corresponding unambiguously to fragments expected for a Cys20–Cys38 (CysIII–CysVI) bond. Analysis of cleavage fragments from peak 3 suggested the presence of two isoforms of singly reduced toxin. The major ions (*m/z* 2741.71 and 1475.11) corresponded to cleavages at Cys6 and Cys30 (CysII–CysIV), while peptide 3772.86 indicated the reduction and cleavage of a Cys4–Cys37 (CysI–CysV) bond. See online Supplementary data for more details.

APETx2 has the same disulfide arrangement (CysI–CysV, CysII–CysIV, CysIII–CysVI) as BDS-I, the only toxin with high homology to APETx2 for which the disulfides have been deduced (NMR data) (Driscoll *et al*, 1989b). Alternative disulfide bond pairings observed in other sea anemone toxins (HmK: I–VI, II–IV, III–V), or inhibitor cystine knot (ICK) toxins (I–IV, II–V, III–VI) were not supported by experimental data.

### *Toxin structure*

Examination of the three-dimensional structures of BDS-I, APETx1, and APETx2 reveals that they share very similar

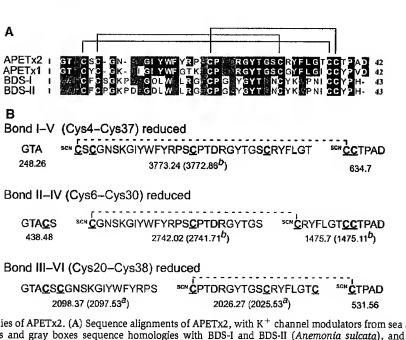


**Figure 1** Structural properties of APETx2. (**A**) Sequence alignments of APETx2, with $K^+$ channel modulators from sea anemones. Black boxes indicate sequence identities and gray boxes sequence homologies with BDS-I and BDS-II (*Anemonia sulcata*), and APETx1 (*Anthopleura elegantissima*). The three disulfide bonds of APETx2, determined by the partial reduction/cyanylation method, are indicated. (**B**) Expected cleavage fragments of APETx2 and their calculated masses (average mass, M+H+) for singly reduced bonds according to the predicted disulfide bond arrangement. The masses in parenthesis were those observed after cleavage and reduction of peak 2[a] and peak 3[b].

features, comprising a triple antiparallel β-sheet motif stabilized by three disulfide bridges. Although the orientation of the N-terminal and connecting loops varies between BDS-I and the APETx toxins, the main differences appear in the surface features. Comparison of BDS-I and APETx1 (Figure 2A, boxed panel) shows that the differences in the primary sequence and therefore amino-acid side chains are primarily reflected on the face of the toxin formed by the N-terminal loop and the last two strands of the β-sheet. APETx1 shows a higher abundance of aromatic residues. Comparison of the differences between APETx1 and APETx2 (Figure 2A) shows that differences in sequence result mostly in surface variations on the opposite side of the toxin and to a lesser extent in the C-terminal area. Of particular significance are the replacements in APETx2 of Tyr5, Lys8, and Ileu10 by Ser5, Asn8, and Lys10, respectively, and the replacement of Gly16, Thr17, and Pro18 by Tyr16, Arg17, and Lys18. The latter induce a tighter turn of the loop connecting the first and second strands of the β-sheets due to Pro18, and comprise a surface that is at the same time bulkier (Tyr16) and bears more positive charges (Figure 2B). The replacement of Gly31 by Arg 31 also contributes to the constitution of a strong basic patch on this side of the toxin. The modifications on the opposite side of the toxin result in a more negatively charged patch, surrounded by an area of hydrophobic or neutral residues. Comparison with BDS-I (Figure 2B) shows that this area is significantly different, and thus may play a role in channel selectivity. The main differences between APETx1 and APETx2 appear to be located on two opposite sides of the molecule, with the β-turn composed of Tyr16, Arg17, and Lys18, which could be hypothesized as a significant selectivity site for recognition of ASIC3.

### *APETx2 inhibits homomeric ASIC3 current*

Rat homomeric ASIC3 currents induced every minute by a rapid step to pH 6 from pH 7.4 were recorded from *Xenopus* oocytes (Figure 3A, ▲) or COS cells (Figure 3A, ●). Toxin-containing solutions at pH 7.4 were perfused before the acidic step. Inhibition of the ASIC3 current started at 10 nM APETx2 and was maximal at 3 μM (Figure 3A and B). The inhibition of ASIC3 currents was rapid and saturated within 30 s of APETx2 perfusion. The concentration–response relationship indicates an $IC_{50}$ of 63 nM (Figure 3A). Effects were totally reversible within 4 min (Figure 3C). The sustained component of ASIC3 current, easily measurable at pH 4, was insensitive to 3 μM APETx2, even though the transient peak component was totally inhibited (Figure 3D).

Human ASIC3 expressed in COS cells was also inhibited by APETx2 with an $IC_{50}$ of 175 nM and $n_H$ of 1 (not shown).

APETx2 (3 μM) perfused for 30 s before the pH drop did not significantly inhibit ASIC1a, ASIC1b, or ASIC2a homomeric currents activated at pH 6 or 5 ($n = 5$–6 cells under each condition, $P > 0.05$, not shown) and expressed in COS cells.

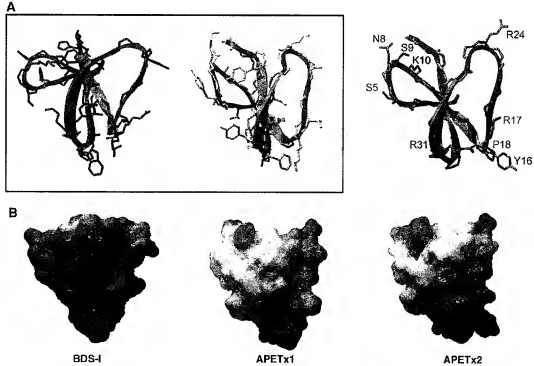


**Figure 2** Molecular modeling of APETx2. (A) Ribbon representations of BDS-I, APETx1, and APETx2. Peptide backbones and selected side chains are superimposed on the ribbon structure. To compare the models of BDS-I and APETx1 (box), only side chains of nonconserved amino acids are apparent. The model of APETx2 shows side chains differing between APETx1 and APETx2, and Arg24, which could be part of the active site of the toxin. (B) Surface representation of the same toxins, mapped with the calculated electrostatic potential distribution (Blue = positive, red = negative, white = neutral) showing the charge distribution on the calculated toxin surface. All structures were generated with DeepView v3.7 and raytraced in PovRay.

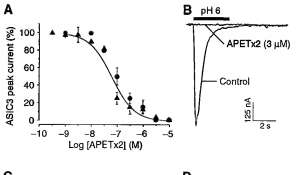


**Figure 3** Effect of APETx2 on homomeric ASIC3 current. (**A**) Concentration-response curve for APETx2 effects on ASIC3 channels expressed in *Xenopus* oocytes (▲) and in COS cells (●). Holding potential: −50 mV, pH drop from 7.4 to 6. APETx2 was perfused for 30 s before the pH drop. Data were fitted by the Hill equation ($n_H = 1$) giving an $IC_{50}$ value of 63 nM. Each point is the mean ± s.e.m. (3–6 cells). (**B**) APETx2 (3 μM) totally inhibits the ASIC3 current. (**C**) Effect of 100 nM APETx2 on ASIC3 currents, and reversibility. (**D**) Upon stimulation of ASIC3 at pH4, APETx2 (3 μM) inhibits the peak, but not the plateau phase of the current.

### *APETx2 directly inhibits homomeric ASIC3 channels in outside-out patches*

Unitary ASIC3 currents triggered by an external pH drop from 7.4 to 6.6 were recorded at −50 mV from outside-out patches of transfected COS cells. A high number of channels were usually simultaneously recorded even when submaximally activated at pH 6.6 (Figure 4A). When APETx2 (3 μM) was applied to the bath solution 30 s before the pH drop, it induced a 75 ± 6% ($n = 4$) inhibition of ASIC3 peak current and this effect was rapidly reversible. Amplitude histograms obtained from the analysis of ASIC3 unitary current recorded before (Figure 4Ba) and after (Figure 4Bb) application of APETx2 show that the unitary amplitude of ASIC3 currents was not modified by the toxin. The mean amplitude values are shown in Figure 4C. These results show that the ASIC3 channel is directly inhibited by the toxin, without any change in its unitary conductance. Similar results were obtained with 100 nM APETx2 producing a partial inhibition of the peak outside-out current (58 ± 7%).

### *Effects of APETx2 on the heteromeric ASIC1a + 3 current*

As ASIC1a and ASIC3 channels are co-localized in sensory neurons (Voilley *et al*, 2001; Alvarez de la Rosa *et al*, 2002), we studied the effects of APETx2 on the heteromeric ASIC1a + 3 channel expressed in COS cells using the pBudCE4.1 vector designed for simultaneous expression of two genes under the control of two independent promoters. The current induced at pH 5 exhibits ASIC3-like kinetics and a plateau phase (Figure 5Aa). The inactivation time constant, 258 ± 136 ms ($n = 8$), was comparable to that of the ASIC3 current (440 ± 135 ms, $n = 15$). As shown previously (Escoubas *et al*, 2000a), this current was insensitive to 10 nM PcTx1, a concentration that completely blocks the homomeric ASIC1a current (Figure 5Ab). The ASIC1a + 3 current induced at pH 6 was only partly inhibited (63 ± 10%, $n = 6$) by high concentrations of APETx2 (3 μM). Moreover, the ASIC1a + 3 current appears to be less sensitive than homomeric ASIC3 current, with an $IC_{50}$ of 2 μM ($n_H = 0.9$; Figure 5D, ○).

### *Effects of APETx2 on the heteromeric ASIC1b + 3 current*

The ASIC1b channel is expressed in small- and large-diameter sensory neurons (Chen *et al*, 1998; Alvarez de la Rosa *et al*, 2002; Mamet *et al*, 2002). Co-expression of ASIC1b + 3 subunits in COS cells using the pBudCE4.1 vector resulted in channels carrying a rapidly activating and inactivating current at pH 6, with an inactivation time constant of 346 ± 183 ms ($n = 20$), comparable to that of the ASIC3 current (440 ± 135 ms, $n = 15$, Figure 5C). A plateau phase was recorded at pH 5 and pH 4. Similar to the ASIC1a + 3 current, the ASIC1b + 3 current was inhibited by APETx2, but with a lower affinity than the ASIC3 current ($IC_{50} = 0.9$ μM, $n_H = 0.9$) (Figure 5D, ■).

### *Effects of APETx2 on the heteromeric ASIC2b + 3 current*

Both ASIC2b and ASIC3 are expressed in small- and large-diameter sensory neurons (Lingueglia *et al*, 1997; Voilley *et al*, 2001; Alvarez de la Rosa *et al*, 2002). Their coexpression in heterologous systems results in channels activated at acidic pH with a transient $Na^+$-selective current, followed by a sustained nonselective cation current (Lingueglia *et al*, 1997). The ASIC2b + 3 sustained current can be recorded as an inward plateau at −50 mV (Figure 5Ba), and as an outward steady-state current at +30 mV and above (Figure 5Bb). Independently of the holding potential, only the peak ASIC2b + 3 current was inhibited by increasing concentrations of APETx2 (Figure 5Ba and b), with an $IC_{50}$ of 117 nM ($n_H = 1$, Figure 5D, ●).

### *Effects of APETx2 on the heteromeric ASIC2a + 3 current*

ASIC2a has been shown to be mainly expressed in medium- and large-diameter sensory neurons (Garcia-Anoveros *et al*, 2001; Alvarez de la Rosa *et al*, 2002) and has not been shown to be involved in nociceptor function. However, its contribution to native currents cannot be excluded as low ASIC2a levels have been detected in rat sensory neurons (Voilley *et al*, 2001; Alvarez de la Rosa *et al*, 2002). The ASIC2a + 3 current recorded in transfected COS cells shows a typical biphasic current with a transient phase, followed by a plateau (Babinski *et al*, 2000; Baron *et al*, 2001). APETx2 (3 μM) blocked neither the rapid nor the slow component of the ASIC2à + 3 current (not shown, $n = 5$).

### *Effects of APETx2 on $K^+$ channels*

Due to its sequence homology with the BDS toxins and APETx1, APETx2 was tested on various heterologously expressed Kv channels. None of them (Kv1.4, HERG, Kv2.2, Kv3.1, Kv4.1, Kv4.2, Kv4.3) was significantly inhibited by

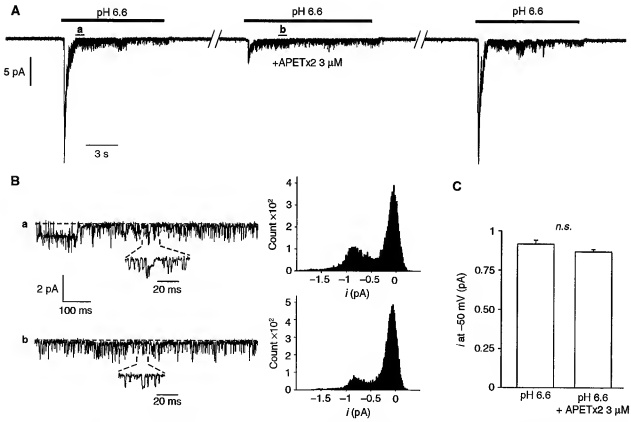


**Figure 4** Effect of APETx2 on unitary ASIC3 currents recorded from outside-out patches. ASIC3 currents were recorded from COS transfected cells. Holding potential: −50 mV, pH drop from 7.4 to 6.6. (**A**) Inhibitory effect of APETx2 (3 μM) on an ASIC3 current recorded from a single excised patch. The current was triggered every minute, and APETx2 was externally applied 30 s before the second pH drop. The inhibition of ASIC3 current was 75±6% ($n=4$), and reversible. (**B**) Time-scale magnifications of parts of current trace shown in (A) (see a and b), and amplitude histograms of unitary current recorded before (a) and after (b) the application of APETx2. (**C**) Statistical analysis of ASIC3 unitary current amplitude measured at −50 mV in the presence and in the absence of APETx2 (4 excised patches, *n.s.*, nonsignificant).

300 nM APETx2. Only the Kv3.4 current was partially inhibited by much higher concentrations (3 μM) of APETx2 (38±2%, $n=6$, not shown).

### *APETx2 inhibits ASIC3-like currents in primary cultures of rat sensory neurons*

ASIC3-like currents were selected for their lack of sensitivity (less than 20% inhibition) to PcTx1 (Escoubas *et al*, 2000a), and for their typical kinetics and pH dependency (Mamet *et al*, 2002). Among the DRG neurons recorded, 26.5% expressed a PcTx1-resistant ASIC3-like current. This biphasic current could show either a $Na^+$-specific current as expected for homomeric ASIC3 channels, or a nonspecific sustained cation current, probably flowing through heteromeric ASIC2b+3 channels (Lingueglia *et al*, 1997) (Figure 6A). Neurons expressing a 10 μM capsaicin-activated VR1 current were excluded. As shown by current traces in Figure 6B, APETx2 inhibited the ASIC3-like current of sensory neurons in a concentration-dependent manner when applied before the pH drop. However, the current was not fully inhibited by the toxin and 3 μM APETx2 reduced the ASIC3-like current amplitude to 51±3% ($n=11$) of the control. The sigmoidal fit of the concentration-dependent inhibition of the ASIC3-like current by APETx2 shows an $IC_{50}$ of 219 nM (Figure 6C). A mean $IC_{50}$ of 216±49 nM ($n=6$) was calculated from $IC_{50}$ values obtained from six different neurons. The effect of APETx2 was the same whether the ASIC3-like current was activated at pH 6.3 or pH 5 (not shown).

Experiments have been performed on ASIC-like current recorded from sensory neurons of ASIC3 knockout adult mice (52 neurons, two primary cultures). These neurons do not express ASIC3-like current. No ASIC2-like current was recorded, consistent with previous observations that ASIC2a is essentially not expressed in DRG neurons (Lingueglia *et al*, 1997; Mamet *et al*, 2002). In 15% of recorded $ASIC3^{-/-}$ DRG neurons, an ASIC1-like current was recorded, which was blocked by the ASIC1a-specific toxin PcTx1 (10 nM), but resistant to APETx2 (3 μM). This result is in agreement with the absence of inhibition of the recombinant ASIC1a current by APETx2.

APETx2 shares about 40% sequence homology with the *Anthopleura* sp. toxins, which are potent activators of voltage-dependent $Na^+$ channels (Romey *et al*, 1976; Kodama *et al*, 1981; Schweitz *et al*, 1981; Reimer *et al*, 1985). Therefore, we tested the effect of APETx2 on action potential triggering in sensory neurons. Figure 6D shows membrane potential variations induced by two current pulses, one infraliminar and the other reaching the action potential threshold, in the absence (top) and presence of 1 μM APETx2 (bottom) on the same neuron. APETx2 did not

 

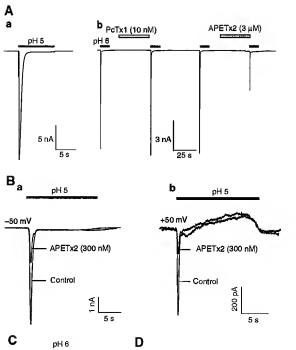


**Figure 5** Effect of APETx2 on heteromeric ASIC1a + 3, ASIC1b + 3, and ASIC2b + 3 channels. ASIC subunits were co-expressed in COS cells. Drugs were perfused for 30 s before the pH drop, as indicated above each current trace. (**A**) ASIC1a + 3 current stimulated at pH 5 exhibits a peak and a plateau phase (a). At pH 6, the current is insensitive to PcTx1 (10 nM), whereas partly inhibited by APETx2 (3 μM) (b). (**B**) The peak ASIC2b + 3 current is inhibited by 300 nM of APETx2 (a) (HP = −50 mV). At +50 mV, the peak ASIC2b + 3 current was also inhibited by the toxin (b), whereas the outward sustained phase was insensitive to APETx2 (300 nM). (**C**) The heteromeric ASIC1b + 3 current was half-inhibited by 1 μM APETx2 (HP = −50 mV). (**D**) Concentration-response relationship for APETx2 block of ASIC2b + 3 (●), ASIC1b + 3 (■), and ASIC1a + 3 (○) currents. The concentration-response curve was fitted by the Hill equation. The $IC_{50}$ values are 117 nM, 0.9 μM, and 2 μM ($n_H$ of 1, 0.9, and 0.9) for ASIC2b + 3, ASIC1b + 3, and ASIC1a + 3, respectively. Each point is the mean ± s.e.m. of data from three to eight cells.

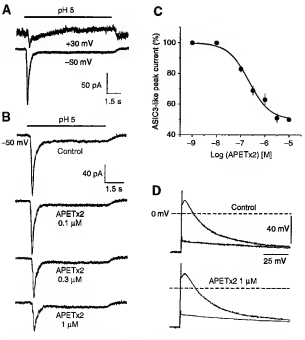


**Figure 6** Effect of APETx2 on ASIC3-like current in primary cultures of rat sensory neurons. (**A**) Original current traces of an ASIC2b + 3-like current showing typical ASIC3-like kinetics at the holding potential of −50 mV and an outward sustained cation current at + 30 mV. (**B**) Original current traces of ASIC3-like current in the absence (control) and in the presence of increasing concentrations of APETx2 applied before the pH drop. This neuron expressed no VR1 current and the ASIC3-like current showed a cation nonselective plateau phase (outward current at + 30 mV, not shown). In this neuron, the ASIC3-like current was maximally inhibited by 1–3 μM APETx2 to 47% of the control amplitude, and the fit of the concentration-dependent block showed an $IC_{50}$ = 203 nM. (**C**) Concentration–response curve of APETx2 inhibition of ASIC3-like current. The amplitude of the current in the presence of toxin was expressed as a percentage of the amplitude of control current and plotted as a function of toxin concentration. Each point is the mean ± s.e.m. of data from 5–17 cells. $IC_{50}$ = 219 nM, $n_H$ = 1. (**D**) Current-clamp recordings of membrane potential variations induced by the same current pulses in control (top) and in the presence of 1 μM APETx2 (bottom) on the same neuron. Two potential traces are shown under each condition: one induced by an infraliminar current pulse and the other induced by a supraliminar current pulse inducing an action potential firing. APETx2 does not significantly modify action potential triggering or kinetics.

significantly modify the action potential triggering or its kinetics, eliminating the possible nonspecific effects on voltage-dependent $Na^+$ and $K^+$ channels involved in the action potential of sensory neurons.

### *In vivo central injections of APETx2*

Central injections of APETx2 in mice were administered to evaluate the toxicity and/or possible behavioral changes. Intracisternal injections of 5, 10, and 20 μg of APETx2 did not induce neurotoxic symptoms in mice even after 24 h. The behavior of injected mice was identical to that of control mice injected with physiological solution.

## Discussion

Animal venoms have provided a great variety of toxins, which have been successfully used as tools to characterize ion channels. The emergence of specific pharmacological tools for ASIC channels started with the discovery of Psalmotoxin 1 (PcTx1), a tarantula peptide that blocks with high specificity and affinity homomeric ASIC1a channels (Escoubas *et al*, 2000a, 2003). We have now isolated and characterized APETx2, the first toxin able to inhibit selectively ASIC3-containing channels and ASIC3-like currents in DRG neurons.

APETx2 reversibly inhibited the rat ASIC3 peak current with an $IC_{50} = 63$ nM, as well as the human ASIC3 peak current with an $IC_{50} = 175$ nM. Outside-out patch recording demonstrated that APETx2 directly inhibits the ASIC3 channel, without any change in its unitary conductance. APETx2 also inhibits the heteromeric ASIC2b + 3 channel with an $IC_{50}$ of 117 nM and heteromeric ASIC1a + 3 and ASIC1b + 3 channels with lower affinities ($IC_{50} = 2$ and 0.9 μM, respectively).

Similar to amiloride, which has been shown to inhibit ASIC3 with an $IC_{50} = 63$ μM (Waldmann *et al*, 1997a), APETx2 blocks the peak ASIC3 current without affecting the sustained plateau. Analysis of structure–function relationships of the FaNaC channel, another member of the ENaC/ASIC family (Lingueglia *et al*, 1995), has previously shown that amiloride blocks the channel by entering into the pore structure (Poet *et al*, 2001).

Although APETx2 has sequence homologies with the *Anthopleura* sp. toxins (AP-A, AP-B, AP-C), which are potent activators of voltage-dependent $Na^+$ channels (Romey *et al*, 1976; Kodama *et al*, 1981; Schweitz *et al*, 1981; Reimer *et al*, 1985), it does not modify the triggering or kinetics of the action potential in rat sensory neurons, thus showing no nonspecific effect on voltage-dependent $Na^+$ channels. This is not surprising as APETx2 was purified from a sea anemone peptide fraction devoid of paralytic activity (Bruhn *et al*, 2001). APETx2 was also non-toxic to mice after i.c. injection using doses 100–1000-fold higher than the known $LD_{50}$ for AP-A (AxI) or AP-B (AxII) administered under the same conditions (Schweitz, 1984). Furthermore, the basic residues (Arg 12, Arg14, Lys 48, or Lys49 in AP-A or AP-B), which have been implicated in the toxin interaction with $Na_v$ channels (Barhanin *et al*, 1981; Gallagher and Blumenthal, 1994; Khera and Blumenthal, 1994; Loret *et al*, 1994), are absent in the APETx2 primary sequence. Similarly, hydrophobic (Trp 33 in AP-B) or acidic residues (Asp7, Asp9 in AP-B), also implicated in toxin binding to the $Na_v$ channel (Dias-Kadambi *et al*, 1996; Khera and Blumenthal, 1996), are absent in APETx2.

The structure of APETx2 is more closely related to that of the $K^+$ channel modulators BDS-I, BDS-II, and APETx1, purified, respectively, from *Anemonia sulcata* and *Anthopleura elegantissima* (Driscoll *et al*, 1989a, b; Diochot *et al*, 1998, 2003). These short polypeptides are folded into three-stranded antiparallel β-sheets connected by three disulfide bonds whose location is similar to that of the long sea anemone $Na_v$ toxins (Norton, 1991; Loret *et al*, 1994). Although APETx2 shares 57, 55, and 76% sequence homologies with BDS-I, BDS-II, and APETx1, and has the same structural fold, its biological target is different. BDS-I and BDS-II are specific inhibitors of Kv3.4 channels, while APETx1 is a specific blocker of HERG $K^+$ channels. Despite sequence homology with APETx1, the inhibitory effect of APETx2 appears to be specific for ASIC3-containing channels. Toxin structure comparison reveals a highly conserved three-dimensional scaffold, and also two toxin areas that are significantly altered by amino-acid substitutions, probably leading to the different pharmacological profiles. As previously observed for other animal toxins, a similar scaffold is used as a basis for 'combinatorial chemistry', and slight alterations of toxin structure guide the selectivity toward different cellular receptors.

*In vivo*, ASIC-like currents are the result of both homomeric and heteromeric associations of ASIC subunits (Bassilana *et al*, 1997; Babinski *et al*, 2000; Alvarez de la Rosa *et al*, 2002). In order to determine their respective contribution, tools are required that block heteromeric as well as homomeric channels. To this end, APETx2 is the first toxin known to inhibit homomeric ASIC3 channels in addition to several ASIC3-containing heteromers, and thus represents a major pharmacological step in dissecting the molecular basis of acid-induced currents in sensory neurons.

ASIC1a, ASIC1b, ASIC2b, and ASIC3 are often co-expressed in sensory neurons (Lingueglia *et al*, 1997; Waldmann and Lazdunski, 1998; Alvarez de la Rosa *et al*, 2002; Mamet *et al*, 2002), and the inhibition of ASIC3-like current by APETx2 could result from a combination of the various effects of APETx2 on the different ASIC3-containing channels. The existence of ASIC2b + 3 channels is identified by the nonspecific sustained cation current that can often be recorded following the transient ASIC3-like peak (Figure 6A). ASIC1a + 3 and ASIC1b + 3 channels could also participate in the ASIC3-like current, because their electrophysiological properties (activation and inactivation kinetics, plateau phase) cannot distinguish them from the ASIC3 homomeric channel. The presence of ASIC2a + 3 channels is also possible as ASIC2a has now been identified in rat sensory neurons (Voilley *et al*, 2001; Alvarez de la Rosa *et al*, 2002), but the participation of homomeric ASIC2a channels can be ruled out in these experiments due to the low pH sensitivity of these channels ($pH_{0.5} = 4.4$, (Lingueglia *et al*, 1997; Baron *et al*, 2001)). As neurons expressing capsaicin-sensitive VR1 current were excluded and homomeric ASIC1a current were blocked by PcTx1, the partial inhibitory effect of APETx2 on ASIC3-like current in sensory neurons could then result from an inhibition of ASIC3 and ASIC2b + 3 channels, in addition to a very partial inhibition of ASIC1a + 3 and ASIC1b + 3 channels.

The discovery of a toxin with ASIC3-blocking activity is of major significance given the substantial amount of evidence now implicating this channel in the transduction of acid-induced pain and hyperalgesia. ASIC3 channel activity is dramatically increased in the presence of lactate (produced under ischemic conditions), and is responsible for sensing and transmitting pain associated with myocardial ischemia (Immke and McCleskey, 2001). ASIC channel expression, particularly ASIC3, is upregulated by proinflammatory mediators including NGF, and has been implicated in sensory neuron hyperexcitability and hyperalgesia (Mamet *et al*, 2002, 2003). In addition, ASIC3 and ASIC3-like currents are potentiated by neuropeptides that are overexpressed under inflammatory conditions (Deval *et al*, 2003).

Two independent groups reported that ASIC3 channels play a role in the modulation of pain sensation (Price *et al*, 2001; Chen *et al*, 2002), and it was recently shown that ASIC3, but not ASIC1, is involved in the development of acid-induced mechanical hyperalgesia in skeletal muscle and central sensitization (Sluka *et al*, 2003). This finding is important for understanding the development of chronic musculoskeletal pain syndromes, and identifies ASIC3 as a potential therapeutic target for treatment or prevention of chronic hyperalgesia. In addition to studies in rat and mouse models, ASIC channels have been shown to be the primary acid sensors in human nociceptors *in vivo* (Ugawa *et al*,

2002). APETx2 is the first and so far the unique peptide toxin inhibitor of ASIC3-containing channels. Along with PcTx1, APETx2 will be an important component of the pharmacological toolbox needed to determine the physiological involvement of ASIC channels in neuronal excitability and pain coding.

## Materials and methods

### *Purification of APETx2 from Anthopleura elegantissima*

A pool of polypeptides was isolated from a crude water–methanol extract of the sea anemone *Anthopleura elegantissima* (Bruhn *et al*, 2001) by anion exchange chromatography on QAE Sephadex A-25 (4.5 × 400 mm) eluted with ammonium acetate (pH8.3), followed by gel filtration on Sephadex G50 (12 × 140 cm) in acetic acid 1 M. Six fractions were tested on ASIC3 channels expressed in *Xenopus* oocytes. One fraction, which inhibited 90% of the ASIC3 current, was further purified by reversed-phase HPLC (Waters Symmetry C18, 4.6 × 250 mm), with a linear gradient from 10 to 40% of solvent B (10% acetonitrile/TFA 0.1%) in 30 min, at 1 ml/min. The separation was carried out on a HP1100 system (Hewlett Packard, USA) coupled to a diode-array detector with UV absorbance monitoring at 220 and 280 nm. The active fraction was then purified on a TSK-SP5PW (7.5 × 75 mm) cation exchange column (Tosoh, Japan) equilibrated in water/acetic acid 1% using a linear gradient from 0 to 100% ammonium acetate 1 M in 50 min at 1 ml/min. Final purification of APETx2 was carried out on the same reversed-phase HPLC column, using a linear gradient from 20 to 30% in 10 min, followed by 30–40% solvent B in 20 min.

### *Peptide sequencing and mass determination*

APETx2 was reduced with 2-mercaptoethanol and alkylated with 4-vinylpyridine prior to N-terminal automated Edman sequencing (477A, Applied Biosystems, USA). The C-terminal sequence of the peptide was confirmed by citraconylation of the arginine residues, followed by trypsin digestion. Tryptic fragments were separated by HPLC (Waters C18, 2 × 150 mm) using a 40 min linear gradient from 5 to 50% of acetonitrile/TFA 0.1% in water/TFA 0.1% at 200 µl/min. Sequence homologies were determined from a BLAST search (http://www.ncbi.nlm.nih.gov/BLAST/). Molecular mass determination was carried out by MALDI-TOF Mass Spectrometry on a Voyager DE-PRO system (Applied Biosystems, USA) in reflector mode, with α-cyano-4-hydroxycinnamic acid matrix (Sigma-Aldrich, USA) and internal calibration. Mass spectra were analyzed with Data Explorer software, and theoretical molecular masses were calculated from sequence data using GPMAW (http://welcome.to/gpmaw/).

### *Disulfide bridge determination*

The disulfide bond arrangement of APETx2 was determined using the partial reduction and cyanylation-induced cleavage method (Wu *et al*, 1996; Qi *et al*, 2001). Briefly, 5 nmol of toxin was dissolved in 5 µl of citrate buffer (0.1 M, pH 3, 6 M guanidine HCl). Partial reduction was carried out by adding 150 nmol of tris(2carboxyethyl)-phosphine hydrochloride (TCEP) and incubating for 20 min at 40°C. Cyanylation was achieved by adding a large excess (4000 nmol, pH 3) of 1-cyano-4-(dimethylamino)pyridinium tetrafluoroborate (CDAP) and incubating for 15 min at room temperature. The mixture was diluted to 200 µl with water/0.1% TFA and separated by reversed-phase HPLC using a linear gradient of 20–40% acetonitrile in water/TFA 0.1% over 40 min (Merck Purospher STAR C18 55 × 4.6 mm, 3 µm). After analysis by MALDI-TOF mass spectrometry, fractions containing singly and doubly reduced isoforms were vacuum-dried and dissolved in 2 µl of 1 M $NH_4OH$ (pH 8, 6 M guanidine HCl), to which was added another 8 µl of 1 M $NH_4OH$ for cleavage (1 h, room temperature). The $NH_4OH$ was removed under vacuum before complete reduction with 2 µl of 0.1 M TCEP (200 mM, citrate buffer, pH 3) for 30 min at 37°C. Samples were desalted on reversed-phase microcolumns (ZipTips C18, Millipore, USA) prior to MALDI-TOF MS analysis.

### *Molecular modeling*

A model of APETx2 was calculated from the previously described coordinates of APETx1 (Diochot *et al*, 2003), using the DeepView Swiss-PDB viewer software v3.7 (http://us.expasy.org/spdbv/). The model was optimized via the Swiss-Model server (http://swissmodel.expasy.org/). BDS-I coordinates (1BDS) were obtained from the PDB database (http://www.rcsb.org/pdb/).

### *Xenopus oocytes preparation, cRNA injections, and electrophysiological measurements*

Oocytes preparation and cRNA injections have been previously described (Diochot *et al*, 1998) (see online Supplementary data). Rat ASIC3 cRNA was synthesized with the mCAP RNA capping kit (Stratagene). A rapid perfusion system allowed local and rapid changes of extracellular solutions. Depending on the pH range, solutions were buffered with HEPES (pH > 6), MES (pH between 6 and 5) or acetate (pH < 5).

### *COS cell transfections*

COS-7 cells were transfected with pCI-rASIC1a, pCI-rASIC1b, pCI-rASIC2a, pCI-rASIC2b, pCI-rASIC3, and pCI-hASIC3 as previously described (Linguegliа et *al*, 1997; Anzai *et al*, 2002). For heteromeric expression, cells were co-transfected with: pCI-rASIC2a and pCI-rASIC3 (1:1 ratio) or pCI-rASIC2b and pCI-rASIC3 (1:1 ratio), and with an expression vector containing the CD8 receptor cDNA, using the DEAE-dextran method. The heteromeric expressions of ASIC1a + 3 and ASIC1b + 3 were achieved using the pBudCE4.1 vector (Invitrogen), which contains the human cytomegalovirus (CMV) immediate-early promoter and the human elongation factor 1α-subunit (EF-1α) promoter for high-level, constitutive, independent expression of two recombinant proteins. Rat ASIC3 (Accession Number # AAB69328) was subcloned under the control of the EF-1α promoter, whereas rat ASIC1a (Accession Number # U94403) or rat ASIC1b (Accession Number # AJ309926) was subcloned under the control of the CMV promoter. $K^+$ channels were expressed using 0.01 µg of pCI-rKv1.4, pCI-rKv2.2, pRc/CMV rKv3.4, 0.05 µg of pCI-rKv4.1, pCI-rKv4.2, pCI-rKv4.3, and pSI-rHERG per dish. Currents in COS-7 cells were recorded at room temperature (22°C) within 1–2 days of transfection.

### *Primary culture of sensory neurons*

Dorsal root ganglia were dissected from Wistar rats (5–7 weeks) and enzymatically dissociated with 0.1% collagenase. Cells were then plated on collagen-coated 35 mm Petri dishes and maintained in culture at 37°C (95% air/5% $CO_2$) in DMEM containing 5% fetal calf serum. Electrophysiological experiments were carried out 1 or 2 days after plating (Mamet *et al*, 2002).

### *Patch-clamp recording*

Currents were sampled at 3.3 or at 20 kHz for whole-cell and outside-out patch-clamp recordings (Hamill *et al*, 1981), and low-pass filtered at 3 kHz using pClamp8 software (Axon Instruments). Off-line analysis of currents was performed using pClamp and BioPatch (Bio-Logic Science Instruments). The pipette solution contained (in mM): KCl 140, NaCl 5, $MgCl_2$ 2, EGTA 5, HEPES-KOH 10 (pH 7.4) and the bath solution contained (in mM): NaCl 140, KCl 5, $MgCl_2$ 2, $CaCl_2$ 2, BSA 0.1%, HEPES-NaOH 10 (pH 7.4). Depending on the pH range, solutions were buffered with HEPES (pH > 6), MES (pH between 6 and 5) or acetate (pH < 5). Solutions were applied locally by a rapid perfusion system. For experiments with sensory neurons, glucose 10 mM, CNQX 20 µM, and kynurenic acid 10 µM (to inhibit glutamate-activated ionotropic currents) were added to the bath solution, and the pipette solution contained (in mM): KCl 140, ATP-$Na_2$ 2.5, $MgCl_2$ 2, $CaCl_2$ 2, EGTA 5, and HEPES 10 (pH 7.3, pCa estimated to 7).

### *Analysis*

Concentration–response curves were fitted by the Hill equation:

$$I = \text{Imax} + (\text{Imin} - \text{Imax})(C^{n_H}/(C^{n_H} + IC_{50}^{n_H}))$$

where $I$ is the amplitude of relative current, Imax is the maximum current amplitude, Imin is the minimum current amplitude, $C$ is the toxin concentration, $IC_{50}$ is the toxin concentration that half-maximally inhibited the current, and $n_H$ is the Hill coefficient. The results are expressed as mean ± standard error of the mean (s.e.m.). Statistical significance was determined using the Student's *t*-test ($P < 0.05$*, $P < 0.01$**, $P < 0.005$***).

***Mouse intracisternal injections***

Anesthetized 5-week-old outbred OF1 (Charles River) mice were injected intracisternally with 1–5 μl APETx2 diluted in sterile NaCl solution (0.9% NaCl, 0.1% BSA). Symptoms were observed during the first hour after injection and at regular intervals over 24 h. Control mice were injected with 5 μl of NaCl solution.

***Supplementary data***

Supplementary data are available at *The EMBO Journal* Online.

## References


Akopian AN, Chen CC, Ding Y, Cesare P, Wood JN (2000) A new member of the acid-sensing ion channel family. *Neuroreport* **11:** 2217–2222

Alvarez de la Rosa D, Zhang P, Shao D, White F, Canessa CM (2002) Functional implications of the localization and activity of acid-sensitive channels in rat peripheral nervous system. *Proc Natl Acad Sci USA* **99:** 2326–2331

Anzai N, Deval E, Schaefer L, Friend V, Lazdunski M, Lingueglia E (2002) The multivalent PDZ domain-containing protein CIPP is a partner of acid-sensing ion channel 3 in sensory neurons. *J Biol Chem* **277:** 16655–16661

Askwith CC, Cheng C, Ikuma M, Benson C, Price MP, Welsh MJ (2000) Neuropeptide FF and FMRFamide potentiate acid-evoked currents from sensory neurons and proton-gated DEG/ENaC channels. *Neuron* **26:** 133–141

Babinski K, Catarsi S, Biagini G, Seguela P (2000) Mammalian ASIC2a and ASIC3 subunits co-assemble into heteromeric proton-gated channels sensitive to Gd3+. *J Biol Chem* **275:** 28519–28525

Babinski K, Le KT, Seguela P (1999) Molecular cloning and regional distribution of a human proton receptor subunit with biphasic functional properties. *J Neurochem* **72:** 51–57

Barhanin J, Hugues M, Schweitz H, Vincent JP, Lazdunski M (1981) Structure–function relationships of sea anemone toxin II from *Anemonia sulcata*. *J Biol Chem* **256:** 5764–5769

Baron A, Schaefer L, Lingueglia E, Champigny G, Lazdunski M (2001) $Zn^{2+}$ and $H^+$ are coactivators of acid-sensing ion channels. *J Biol Chem* **276:** 35361–35367

Bassilana F, Champigny G, Waldmann R, de Weille JR, Heurteaux C, Lazdunski M (1997) The acid-sensitive ionic channel subunit ASIC and the mammalian degenerin MDEG form a heteromultimeric $H^+$-gated $Na^+$ channel with novel properties. *J Biol Chem* **272:** 28819–28822

Benson CJ, Eckert SP, McCleskey EW (1999) Acid-evoked currents in cardiac sensory neurons: a possible mediator of myocardial ischemic sensation. *Circ Res* **84:** 921–928

Bode F, Sachs F, Franz MR (2001) Tarantula peptide inhibits atrial fibrillation. *Nature* **409:** 35–36

Bruhn T, Schaller C, Schulze C, Sanchez-Rodriguez J, Dannmeier C, Ravens U, Heubach JF, Eckhardt K, Schmidtmayer J, Schmidt H, Aneiros A, Wachter E, Beress L (2001) Isolation and characterisation of five neurotoxic and cardiotoxic polypeptides from the sea anemone *Anthopleura elegantissima*. *Toxicon* **39:** 693–702

Chen CC, England S, Akopian AN, Wood JN (1998) A sensory neuron-specific, proton-gated ion channel. *Proc Natl Acad Sci USA* **95:** 10240–10245

Chen CC, Zimmer A, Sun WH, Hall J, Brownstein MJ (2002) A role for ASIC3 in the modulation of high-intensity pain stimuli. *Proc Natl Acad Sci USA* **99:** 8992–8997

Coscoy S, de Weille JR, Lingueglia E, Lazdunski M (1999) The pre-transmembrane 1 domain of acid-sensing ion channels participates in the ion pore. *J Biol Chem* **274:** 10129–10132

de Weille JR, Bassilana F, Lazdunski M, Waldmann R (1998) Identification, functional expression and chromosomal localisation of a sustained human proton-gated cation channel. *FEBS Lett* **433:** 257–260

Deval E, Baron A, Lingueglia E, Mazarguil H, Zajac JM, Lazdunski M (2003) Effects of neuropeptide SF and related peptides on acid sensing ion channel 3 and sensory neuron excitability. *Neuropharmacology* **44:** 662–671

Dias-Kadambi BL, Combs KA, Drum CL, Hanck DA, Blumenthal KM (1996) The role of exposed tryptophan residues in the activity of the cardiotonic polypeptide anthopleurin B. *J Biol Chem* **271:** 23828–23835

Diochot S, Loret E, Bruhn T, Beress L, Lazdunski M (2003) APETx1, a new toxin from the sea anemone *Anthopleura elegantissima*, blocks voltage-gated human ether-a-go-go-related gene potassium channels. *Mol Pharmacol* **64:** 59–69

Diochot S, Schweitz H, Beress L, Lazdunski M (1998) Sea anemone peptides with a specific blocking activity against the fast inactivating potassium channel Kv3.4. *J Biol Chem* **273:** 6744–6749

Driscoll PC, Clore GM, Beress L, Gronenborn AM (1989a) A proton nuclear magnetic resonance study of the antihypertensive and antiviral protein BDS-I from the sea anemone *Anemonia sulcata*: sequential and stereospecific resonance assignment and secondary structure. *Biochemistry* **28:** 2178–2187

Driscoll PC, Gronenborn AM, Beress L, Clore GM (1989b) Determination of the three-dimensional solution structure of the antihypertensive and antiviral protein BDS-I from the sea anemone *Anemonia sulcata*: a study using nuclear magnetic resonance and hybrid distance geometry-dynamical simulated annealing. *Biochemistry* **28:** 2188–2198

England LJ, Imaeda J, Jacobsen R, Craig AG, Gulyas J, Akhtar M, Rivier J, Julius D, Olivera BM (1998) Inactivation of a serotonin-gated ion channel by a polypeptide toxin from marine snails. *Science* **281:** 575–578

Escoubas P, Bernard C, Lambeau G, Lazdunski M, Darbon H (2003) Recombinant production and solution structure of PcTx1, the specific peptide inhibitor of ASIC1a proton-gated cation channels. *Protein Sci* **12:** 1332–1343

Escoubas P, De Weille JR, Lecoq A, Diochot S, Waldmann R, Champigny G, Moinier D, Menez A, Lazdunski M (2000a) Isolation of a tarantula toxin specific for a class of proton-gated $Na^+$ channels. *J Biol Chem* **275:** 25116–25121

Escoubas P, Diochot S, Corzo G (2000b) Structure and pharmacology of spider venom neurotoxins. *Biochimie* **82:** 893–907

Gallagher MJ, Blumenthal KM (1994) Importance of the unique cationic residues arginine 12 and lysine 49 in the activity of the cardiotonic polypeptide anthopleurin B. *J Biol Chem* **269:** 254–259

García-Añoveros J, Samad TA, Zuvela-Jelaska L, Woolf CJ, Corey DP (2001) Transport and localization of the DEG/ENaC ion channel BNaC1alpha to peripheral mechanosensory terminals of dorsal root ganglia neurons. *J Neurosci* **21:** 2678–2686

Grunder S, Geissler HS, Bassler EL, Ruppersberg JP (2000) A new member of acid-sensing ion channels from pituitary gland. *Neuroreport* **11:** 1607–1611

Hamill OP, Marty A, Neher E, Sakmann B, Sigworth FJ (1981) Improved patch-clamp techniques for high-resolution current recording from cells and cell-free membrane patches. *Pflugers Arch* **391:** 85–100

Harvey AL, Rowan EG, Vatanpour H, Fatehi M, Castaneda O, Karlsson E (1994) Potassium channel toxins and transmitter release. *Ann NY Acad Sci* **710:** 1–10

Hugues M, Romey G, Duval D, Vincent JP, Lazdunski M (1982) Apamin as a selective blocker of the calcium-dependent potassium channel in neuroblastoma cells: voltage-clamp and biochemical characterization of the toxin receptor. *Proc Natl Acad Sci USA* **79:** 1308–1312

Immke DC, McCleskey EW (2001) Lactate enhances the acid-sensing $Na^+$ channel on ischemia-sensing neurons. *Nat Neurosci* **4:** 869–870


## Acknowledgements

We thank D Moinier, M Jodar, and V Briet for technical assistance, and Dr L Beress for generously and kindly providing sea anemone extracts. This work was supported by the Centre National de la Recherche Scientifique (CNRS), the Ministère de la Recherche et de la Technologie, the Association pour la Recherche contre le Cancer (ARC), Astra Zeneca AB Research Area CNS/Pain, and the Association Française contre les Myopathies (AFM). LD Rash is supported by an INSERM/NH&MRC fellowship (ID 194470).

Khera PK, Blumenthal KM (1994) Role of the cationic residues arginine 14 and lysine 48 in the function of the cardiotonic polypeptide anthopleurin B. *J Biol Chem* **269:** 921–925
Khera PK, Blumenthal KM (1996) Importance of highly conserved anionic residues and electrostatic interactions in the activity and structure of the cardiotonic polypeptide anthopleurin B. *Biochemistry* **35:** 3503–3507
Kodama I, Shibata S, Toyama J, Yamada K (1981) Electromechanical effects of anthopleurin-A (AP-A) on rabbit ventricular muscle: influence of driving frequency, calcium antagonists, tetrodotoxin, lidocaine and ryanodine. *Br J Pharmacol* **74:** 29–37
Kress M, Zeilhofer HU (1999) Capsaicin, protons and heat: new excitement about nociceptors. *Trends Pharmacol Sci* **20:** 112–118
Krishtal O (2003) The ASICs: signaling molecules? Modulators? *Trends Neurosci* **26:** 477–483
Lingueglia E, Champigny G, Lazdunski M, Barbry P (1995) Cloning of the amiloride-sensitive FMRFamide peptide-gated sodium channel. *Nature* **378:** 730–733
Lingueglia E, de Weille JR, Bassilana F, Heurteaux C, Sakai H, Waldmann R, Lazdunski M (1997) A modulatory subunit of acid sensing ion channels in brain and dorsal root ganglion cells. *J Biol Chem* **272:** 29778–29783
Loret EP, del Valle RM, Mansuelle P, Sampieri F, Rochat H (1994) Positively charged amino acid residues located similarly in sea anemone and scorpion toxins. *J Biol Chem* **269:** 16785–16788
Mamet J, Baron A, Lazdunski M, Voilley N (2002) Proinflammatory mediators, stimulators of sensory neuron excitability via the expression of acid-sensing ion channels. *J Neurosci* **22:** 10662–10670
Mamet J, Lazdunski M, Voilley N (2003) How NGF drives physiological and inflammatory expressions of acid-sensing Ion channel 3 in sensory neurons. *J Biol Chem* **30:** 30
Moczydlowski E, Lucchesi K, Ravindran A (1988) An emerging pharmacology of peptide toxins targeted against potassium channels. *J Membr Biol* **105:** 95–111
Norton RS (1991) Structure and structure–function relationships of sea anemone proteins that interact with the sodium channel. *Toxicon* **29:** 1051–1084
Pan HL, Longhurst JC, Eisenach JC, Chen SR (1999) Role of protons in activation of cardiac sympathetic C-fibre afferents during ischaemia in cats. *J Physiol* **518:** 857–866
Poet M, Tauc M, Lingueglia E, Cance P, Poujeol P, Lazdunski M, Counillon L (2001) Exploration of the pore structure of a peptide-gated $Na^+$ channel. *EMBO J* **20:** 5595–5602
Price MP, McIlwrath SL, Xie J, Cheng C, Qiao J, Tarr DE, Sluka KA, Brennan TJ, Lewin GR, Welsh MJ (2001) The DRASIC cation channel contributes to the detection of cutaneous touch and acid stimuli in mice. *Neuron* **32:** 1071–1083
Price MP, Snyder PM, Welsh MJ (1996) Cloning and expression of a novel brain $Na^+$ channel. *J Biol Chem* **271:** 7879–7882
Qi J, Wu J, Somkuti GA, Watson JT (2001) Determination of the disulfide structure of sillucin, a highly knotted, cysteine-rich peptide, by cyanylation/cleavage mass mapping. *Biochemistry* **40:** 4531–4538
Resh PW, Steen KH (1996) Tissue acidosis in nociception and pain. *Prog Brain Res* **113:** 143–151
Reimer NS, Yasunobu CL, Yasunobu KT, Norton TR (1985) Amino acid sequence of the *Anthopleura xanthogrammica* heart stimulant, anthopleurin-B. *J Biol Chem* **260:** 8690–8693
Romey G, Abita JP, Schweitz H, Wunderer G, Lazdunski M (1976) Sea anemone toxin: a tool to study molecular mechanisms of nerve conduction and excitation–secretion coupling. *Proc Natl Acad Sci USA* **73:** 4055–4055
Schweitz H (1984) Lethal potency in mice of toxins from scorpion, sea anemone, snake and bee venoms following intraperitoneal and intracisternal injection. *Toxicon* **22:** 308–311
Schweitz H, Vincent JP, Barhanin J, Frelin C, Linden G, Hugues M, Lazdunski M (1981) Purification and pharmacological properties of eight sea anemone toxins from *Anemonia sulcata*, *Anthopleura xanthogrammica*, *Stoichactis giganteus*, and *Actinodendron plumosum*. *Biochemistry* **20:** 5245–5252
Shakkottai VG, Regaya I, Wulff H, Fajloun Z, Tomita H, Fathallah M, Cahalan MD, Gargus JJ, Sabatier JM, Chandy KG (2001) Design and characterization of a highly selective peptide inhibitor of the small conductance calcium-activated $K^+$ channel, SkCa2. *J Biol Chem* **276:** 43145–43151
Sluka KA, Price MP, Breese NM, Stucky CL, Wemmie JA, Welsh MJ (2003) Chronic hyperalgesia induced by repeated acid injections in muscle is abolished by the loss of ASIC3, but not ASIC1. *Pain* **106:** 229–239
Sutherland SP, Benson CJ, Adelman JP, McCleskey EW (2001) Acid-sensing ion channel 3 matches the acid-gated current in cardiac ischemia-sensing neurons. *Proc Natl Acad Sci USA* **98:** 711–716
Tytgat J, Chandy KG, Garcia ML, Gutman GA, Martin-Eauclaire MF, van der Walt JJ, Possani LD (1999) A unified nomenclature for short-chain peptides isolated from scorpion venoms: alpha-KTx molecular subfamilies. *Trends Pharmacol Sci* **20:** 444–447
Uchitel OD (1997) Toxins affecting calcium channels in neurons. *Toxicon* **35:** 1161–1191
Ugawa S, Ueda T, Ishida Y, Nishigaki M, Shibata Y, Shimada S (2002) Amiloride-blockable acid-sensing ion channels are leading acid sensors expressed in human nociceptors. *J Clin Invest* **110:** 1185–1190
Voilley N, de Weille J, Mamet J, Lazdunski M (2001) Nonsteroid anti-inflammatory drugs inhibit both the activity and the inflammation-induced expression of acid-sensing ion channels in nociceptors. *J Neurosci* **21:** 8026–8033
Waldmann R, Bassilana F, De Weille JR, Champigny G, Heurteaux C, Lazdunski M (1997a) Molecular cloning of a non-inactivating proton-gated $Na^+$ channel specific for sensory neurons. *J Biol Chem* **272:** 20975–20978
Waldmann R, Champigny G, Bassilana F, Heurteaux C, Lazdunski M (1997b) A proton-gated cation channel involved in acid-sensing. *Nature* **386:** 173–177
Waldmann R, Champigny G, Voilley N, Lauritzen I, Lazdunski M (1996) The mammalian degenerin MDEG, an amiloride-sensitive cation channel activated by mutations causing neurodegeneration in *Caenorhabditis elegans*. *J Biol Chem* 271: 10433–10436
Waldmann R, Lazdunski M (1998) H(+)-gated cation channels: neuronal acid sensors in the NaC/DEG family of ion channels. *Curr Opin Neurobiol* **8:** 418–424
Wu J, Gage DA, Watson JT (1996) A strategy to locate cysteine residues in proteins by specific chemical cleavage followed by matrix-assisted laser desorption/ionization time-of-flight mass spectrometry. *Anal Biochem* **235:** 161–174
Xie J, Price MP, Berger AL, Welsh MJ (2002) DRASIC contributes to pH-gated currents in large dorsal root ganglion sensory neurons by forming heteromultimeric channels. *J Neurophysiol* **87:** 2835–2843